



ALMA MATER STUDIORUM
UNIVERSITÀ DI BOLOGNA

DEPARTMENT OF COMPUTER SCIENCE AND ENGINEERING
Master's Degree in Computer Science

Merkle-tree-based integrity verification protocol for geo-distributed storage systems

Supervisor:
Prof. Özalp Babaoğlu

Author:
Santo Cariotti

Session II
Academic Year 2024/2025

Abstract

This thesis presents an integrity verification protocol for geo-distributed storage that integrates Merkle trees, Raft consensus, and Reed-Solomon coding. It addresses the need for efficient and reliable data integrity verification in environments where nodes may be temporarily offline, overcoming the limitations of traditional checksum-based full file scans.

A prototype was implemented using a purpose-built Rust library to efficiently generate Merkle tree root hashes for entire folders, combined with Raft to ensure consistent metadata coordination across distributed nodes. Experimental evaluation demonstrates that the protocol reliably verifies and localizes data corruption across various scenarios and node conditions, maintaining correctness even under partial cluster availability. Verification time, however, increases with cluster size due to coordination and network overhead.

These results indicate that a Merkle-tree-based architecture coordinated through consensus provides a robust and fault-tolerant foundation for distributed integrity verification, while also suggesting avenues for optimization through concurrency, adaptive file organization, and large-scale deployment.

Sommario

Questa tesi propone un protocollo di verifica dell'integrità per sistemi di storage geo-distribuiti, basato su alberi di Merkle, algoritmo di consenso Raft e codifica Reed-Solomon. Il protocollo consente di garantire verifiche dei dati efficienti e affidabili anche in ambienti in cui i nodi possono essere temporaneamente offline, superando i limiti delle tradizionali scansioni di file completi basate su checksum.

Un prototipo è stato implementato tramite una libreria Rust dedicata, capace di generare in modo efficiente gli hash delle radici degli alberi di Merkle per intere cartelle, integrata con Raft per assicurare la coerenza dei metadati tra i nodi distribuiti. La sperimentazione dimostra che il protocollo verifica e localizza in modo affidabile la corruzione dei dati in diversi scenari, mantenendo correttezza anche in caso di disponibilità parziale del cluster. Il tempo di verifica, però, aumenta con la dimensione del cluster a causa dei costi di coordinazione e del sovraccarico di rete.

I risultati indicano che un'architettura basata su alberi di Merkle, coordinata tramite consenso, offre una soluzione robusta e tollerante ai guasti per la verifica distribuita dell'integrità dei dati, suggerendo al contempo possibilità di ottimizzazione attraverso concorrenza, organizzazione adattiva dei file e deployment su larga scala.

Contents

1	Introduction	5
1.1	Motivation	5
1.2	Problem Statement	6
1.3	Research Objectives	6
1.4	Structure of the Document	7
2	Background	8
2.1	Merkle Trees	8
2.1.1	Merkle proofs	9
2.1.2	Applications	11
2.1.3	Alternative Implementations	11
2.2	Cryptographic Hash Functions	12
2.2.1	SHA-256	12
2.2.2	Keccak-256	13
2.2.3	BLAKE3	13
2.3	Consensus Protocols	15
2.3.1	Raft	16
2.3.2	Flutter+Blink	17
2.3.3	Practical Byzantine Fault Tolerance (PBFT)	17
2.3.4	PB-Raft: A Byzantine Extension of Raft	18
2.3.5	Summary	19
2.4	Reed-Solomon	19
2.4.1	Classical Reed-Solomon coding	19
2.4.2	Cubbit's adaptation	20
3	Architecture	21
3.1	Merkle Tree Library	21
3.2	File organization	28
3.2.1	Storing different Merkle trees for each agent	29
3.3	A Raft Cluster for File Uploads	33

3.3.1	Corruption Check	36
3.3.2	Corruption Check for Partial Uploads	36
3.3.3	Recovery of Missing Shards	41
4	Implementation and Tests	43
4.1	Files in a Raft Cluster	43
4.1.1	Gateway service	44
4.1.2	Agent service	46
4.2	Testing Environment and Results	50
5	Conclusion	57
	Bibliography	60
	Appendix	60
A	Listings	i
A.1	Protobuf definition for Agent service	ii
A.2	Gateway Upload Handler Implementation	iii
A.3	SendShard RPC Wrapper Implementation	iv
A.4	Gateway Download Handler Implementation	v
A.5	Agent Service Initialization and gRPC Server Setup	vi
A.6	Raft Node Initialization	vii
A.7	Client-Side Raft Join Request	viii
A.8	Server-Side Raft Join Handler	ix
A.9	Server-Side SendShard Handler	x
A.10	Server-Side GetShard Handler	xi
A.11	Raft Log Command Structure	xi
A.12	Server-Side AckShard Handler	xii
A.13	Raft Log Entry Helper Functions	xiii
A.14	Merkle Tree Creation in Rust	xiv
A.15	Merkle Proof Verification in Rust	xiv
A.16	Merkle Tree Module Prototypes (Go)	xv
A.17	Corruption Check Algorithm	xvi

1 Introduction

This thesis emerged from a practical problem encountered during the development of a modern cloud storage: how can a geo-distributed storage system efficiently detect data corruption without assuming that all nodes are always online? The answer, as explored in this work, lies in rethinking corruption detection through the use of hierarchical data structures and consensus algorithms.

1.1 Motivation

File corruption can silently compromise stored data, reduce reliability, or increase recovery costs. Traditional approaches such as checksums, replication, or RAID [1] provide partial solutions, but they also show limitations when applied to large-scale and geo-distributed environments. In particular, these methods often assume constant node availability or require full scans that become increasingly expensive as data grows.

During my internship at Cubbit¹, the first geo-distributed cloud storage provider, I studied the company's existing integrity verification protocol, which relies on checksum-based verification. While functional, this approach has two key weaknesses: it assumes that nodes are always online, and it requires heavy operations to verify integrity. Moreover, Cubbit stores files using Reed-Solomon coding, meaning that data is distributed into shards across multiple agents, and files are reconstructed from subsets of those shards. This introduces additional challenges, since nodes holding useful shards may be offline at any time.

Motivated by these challenges, I explored an alternative approach based on Merkle trees. Merkle trees, widely used in blockchain and distributed databases, allow efficient and hierarchical verification of large datasets: instead of re-checking entire files, integrity can be confirmed by verifying only a logarithmic number of hashes along a path in the tree. Combined with a consensus algorithm, this structure allows folder-level integrity verification even in clusters where nodes frequently join and leave.

¹<https://cubbit.io>

1.2 Problem Statement

Verifying file integrity at the file level quickly becomes inefficient as the dataset grows. In Cubbit’s environment, the problem is further complicated by node churn: data may be temporarily unavailable, yet the system must still guarantee correctness.

Cubbit’s use of Reed-Solomon coding ensures that files can be reconstructed even when some shards are missing or corrupted. However, Reed-Solomon alone does not provide a way to verify the integrity of individual shards. This means that a reconstructed file could include corrupted data without the system being able to detect where the corruption occurred.

Merkle trees address this gap, providing an efficient mechanism to detect and localize corruption by verifying a logarithmic number of hashes along an authentication path. The key challenge lies in constructing and verifying Merkle trees in a distributed setting, where some shards are stored on agents that may be offline.

This thesis addresses the need for an integrity verification protocol that:

- avoids repeated full file scans by verifying integrity at the folder and sub-folder level;
- tolerates offline nodes by storing and synchronizing integrity metadata across the cluster;
- integrates with Cubbit’s existing Reed-Solomon coding, ensuring that verification is possible even during partial uploads and recoveries.

The central question is: how can a Merkle-tree-based integrity verification protocol, combined with Raft consensus and compatible with Reed-Solomon coding, provide efficient, scalable, and fault-tolerant integrity verification in a geo-distributed cluster?

1.3 Research Objectives

The primary objective of this thesis is to design and evaluate an integrity verification protocol for distributed storage clusters that is both efficient and resilient to node failures. Unlike checksum-based approaches, the proposed system leverages:

- an ad hoc Merkle tree library optimized for folder-based hierarchies;
- coordination via Raft consensus to ensure consistent integrity metadata across nodes;

- integration with Cubbit’s Reed-Solomon-based infrastructure to handle partial uploads and recoveries;

The overarching goal is to demonstrate that an optimized, folder-oriented Merkle tree, combined with consensus, can provide a scalable, fault-tolerant, and efficient alternative to classical checksum-based corruption detection in geo-distributed clusters.

1.4 Structure of the Document

This document is organized as follows:

Chapter 2 provides the necessary background and serves as a literature review. It examines the key technologies and theoretical foundations relevant to this work, including Merkle trees, cryptographic hash functions, consensus algorithms, and the core component of the Cubbit infrastructure. For each of these elements, different solutions proposed in the literature are analyzed and compared. The chapter then introduces the selected solutions, together with the rationale for their adoption, explaining why they are best suited to the integrity verification protocol under consideration.

Chapter 3 describes the architecture of the proposed integrity verification protocol. It explains how the components introduced in Chapter 2 are combined and how they interact within the overall design.

Chapter 4 presents the prototype implementation and the experimental evaluation. The system is tested under different scenarios, varying both the number of agents in the cluster and the number of files stored per agent. Controlled corruption is deliberately injected into the data, and the evaluation measures the elapsed time between the initiation of a corruption check and the correct identification of the corrupted file.

Chapter 5 concludes the thesis by summarizing the main contributions, highlighting limitations, and outlining possible directions for future work.

2 Background

This chapter is intended to provide the reader with some background information on the technologies used in writing this thesis project.

Some of them are essential to better know why the given Merkle tree solution is useful and works for Cubbit's infrastructure.

2.1 Merkle Trees

Merkle trees [2] are a fundamental data structure first introduced by R. Merkle in his PhD dissertation. This section presents the theoretical foundations of Merkle trees, their construction, their practical applications, and the rationale for the implementation chosen in this thesis.

A Merkle tree is a binary tree T of height H with 2^H leaves and $2^H - 1$ internal nodes. Each leaf stores the cryptographic hash of the underlying data, rather than the raw data itself. The same cryptographic hash function is applied recursively at internal nodes, which store the hash of the concatenation of their two children. For a more detailed discussion of collision resistance in cryptographic hash functions, see [3].

Formally, given two child nodes n_{left} and n_{right} , their parent node is defined as:

$$n_{\text{parent}} = f(n_{\text{left}} || n_{\text{right}}) \quad (2.1)$$

where $||$ denotes bit-string concatenation and f is a cryptographic hash function.

Consider now a Merkle tree of height $H > 2$. A leaf node is indexed by $\phi \in \{0, \dots, 2^H - 1\}$. A node at height h and position j (counting from left to right) is denoted as $y_h[j]$, where $h = 0, \dots, H$ and $j = 0, \dots, 2^{H-h} - 1$. Given a cryptographic hash function $f : \{0, 1\}^* \mapsto \{0, 1\}^n$, the recursive definition of an internal node is:

$$y_h[j] = f(y_{h-1}[2j] || y_{h-1}[2j + 1]). \quad (2.2)$$

The root node of the tree, known as the *Merkle root*, serves as a compact commitment to all data contained in the leaves. Because hashes propagate upwards, even a single-bit modification in any leaf causes a change in the root hash.

This property makes Merkle trees powerful tools for integrity verification in large, distributed datasets.

2.1.1 Merkle proofs

One of the most powerful features of Merkle trees is the ability to prove that a given piece of data is part of a larger set, without revealing or recomputing the entire dataset. Given a Merkle tree leaf, one can reconstruct the root by traversing the path to the root and successively combining the node with its siblings.

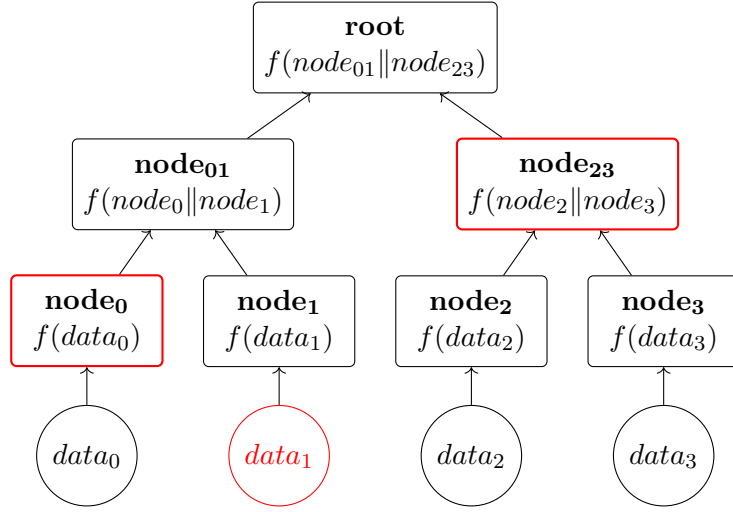


Figure 2.1: Merkle tree authentication path for $data_1$. Leaves are hashed as $node_i = f(data_i)$, and internal nodes are computed as $f(node_{\text{left}} || node_{\text{right}})$ (Equation 2.1). The proof requires only the sibling nodes $\{node_0, node_{23}\}$ to recompute the root.

For each height $h < H$, we define $Auth_h$ to be the value of the sibling node along the path from the leaf to the root. The set of all such siblings $\{Auth_h\}_{h=0}^{H-1}$ is called the *authentication path*. With this path, anyone can recompute the root and verify inclusion by comparing against the published Merkle root.

For instance, Figure 2.1 shows the authentication path corresponding to the second leaf.

This property, known as a *Merkle proof*, enables efficient verification of data integrity. In a naive implementation, the entire Merkle tree is stored in memory. In such a case, generating a proof for a leaf - as illustrated in Algorithm 1 - involves traversing only the path from the leaf to the root. This reduces proof generation from a potentially linear scan of all data ($O(n)$) to a logarithmic traversal of the tree ($O(\log n)$).

Algorithm 1: Merkle proof generation

Input: Leaf index i , full tree levels L_0, L_1, \dots, L_H

Output: Merkle proof π for leaf l_i (or **None** if i invalid)

```
1  $\pi \leftarrow \emptyset$ 
2  $current \leftarrow i$ 
3 foreach  $level \in \{L_0, \dots, L_{H-1}\}$  do
4    $sibling\_index \leftarrow \min(current \oplus 1, |level| - 1)$ 
5    $sibling \leftarrow level[sibling\_index]$ 
6    $position \leftarrow \text{Left}$  if  $sibling\_index < current$ , else Right
7   append  $(sibling.hash, position)$  to  $\pi$ 
8    $current \leftarrow \lfloor current/2 \rfloor$ 
9 end
10 return  $\pi$ 
```

Merkle proof verification algorithm for a proof π is illustrated in Algorithm 2.

Algorithm 2: Merkle proof verification

Input: Data d , proof π , expected root R , hash function f

Output: **true** if valid, **false** otherwise

```
1  $h \leftarrow f(d)$ 
2 foreach  $(sibling, position)$  in  $\pi$  do
3   if  $position = \text{Left}$  then
4      $h \leftarrow f(sibling || h)$ 
5   else
6      $h \leftarrow f(h || sibling)$ 
7   end
8 end
9 return  $h = R$ 
```

Complexity Analysis

- **Proof generation:** $O(\log n)$, because only the sibling nodes along the path from leaf to root are collected.
- **Proof verification:** $O(\log n)$, as each step requires a single hash operation per tree level.
- **Memory:** $O(n)$ to store the full tree in memory, which allows logarithmic-time proof generation.

This approach ensures that Merkle proofs remain efficient even for large datasets, while keeping the implementation simple and compatible with our folder-level integrity checks across a Raft-coordinated cluster.

2.1.2 Applications

Merkle trees are widely used in distributed systems to ensure data integrity:

- **Blockchains:** Bitcoin [4], Ethereum [5], and other systems use Merkle roots to verify transactions efficiently.
- **Version control systems:** Git stores commits as Merkle trees, ensuring history integrity.
- **Distributed storage:** Systems such as IPFS [6] and Amazon DynamoDB [7] use Merkle trees for consistency checks and conflict resolution.

2.1.3 Alternative Implementations

In the literature, several advanced variants of Merkle trees exist, such as XMSS (eXtended Merkle Signature Scheme) [8] and the BDS (Buchmann-Dahmen-Szydlo) traversal algorithm [9]. These schemes were developed in the context of *post-quantum cryptography* and digital signatures. XMSS is standardized by the IETF (RFC 8391) and provides strong security guarantees by organizing one-time signatures (OTS) under a large Merkle tree, where the root of the tree serves as the public key.

In XMSS, to sign a message i , the authentication path of the i -th leaf is needed. In a native way, recomputing this path would require rebuilding large parts of the tree, which becomes impractical when the tree contains millions of leaves. To solve this, the BDS traversal algorithm was introduced: it incrementally maintains and updates the authentication path in $O(h)$ time and $O(h)$ space (where $h = \log_2(n)$ is the tree height). This makes XMSS practical for very large trees.

In our case, however, the scenario is fundamentally different. We are not designing a post-quantum signature scheme but a integrity verification protocol for folders in a geo-distributed storage cluster. The size of our Merkle trees is modest: typically on the order of tens of leaves per folder. For trees of this size:

- Proofs can be recomputed directly, without significant computational overhead.
- The space-time optimizations of BDS provide no practical benefit.

- The additional complexity of XMSS and BDS would introduce unnecessary implementation overhead.

For this reason, this thesis opted for a *simple* Merkle tree implementation, applied independently at the folder and sub-folder level. This keeps the system lightweight, efficient, and easy to integrate with a consensus mechanism. It also avoids the pitfalls of managing very large Merkle trees (as in XMSS) or the stateful requirements of post-quantum signature schemes, which are irrelevant in our use case.

2.2 Cryptographic Hash Functions

In the previous section, Merkle trees were discussed in detail, with particular attention to the use of cryptographic hash functions for node construction. One of the questions that emerged during my internship was: “*what is the fastest cryptographic hash function?*”.

This section explores the motivation behind testing different cryptographic hash functions (SHA-256, Keccak-256, and BLAKE3) within the context of this project and why, among these, BLAKE3 was selected as the primary candidate for benchmarking in this thesis due to its performance and modern design.

2.2.1 SHA-256

SHA-256 is part of the SHA-2 family of cryptographic hash functions, standardized by NIST in 2001 [10]. It produces a 256-bit output from input messages of arbitrary length and is widely used in security protocols such as TLS, digital signatures, and blockchain systems like Bitcoin.

The algorithm processes data in 512-bit blocks using 32-bit words. On 32-bit architectures, this design choice makes SHA-256 relatively efficient. However, on modern 64-bit CPUs, the reliance on 32-bit operations leads to extra instructions, making it slower than SHA-512 and significantly less efficient than more modern designs such as BLAKE3. By contrast, SHA-512 processes 1024-bit message blocks with 64-bit operations, making it more efficient on such architectures. In this thesis, however, SHA-512 was not benchmarked, as the focus was on SHA-256 and the comparison against Keccak-256 and BLAKE3.

Despite these performance limitations, SHA-256 remains a cornerstone in cryptography due to its simplicity, standardization, and lack of practical vulnerabilities. It is often used as a reference point in performance evaluations of newer hash functions.

2.2.2 Keccak-256

Keccak-256 [11] is the 256-bit variant of the Keccak family, which won the NIST SHA-3 competition in 2012 [12]. Unlike SHA-2, Keccak is based on a *sponge construction* that alternates between absorbing input blocks and squeezing output. This design provides strong theoretical guarantees and a high level of security against known cryptanalytic attacks.

Although Keccak-256 is cryptographically very robust, its performance is generally slower than SHA-2 and significantly slower than BLAKE3 in software implementations. However, its adoption is widespread in domains where security guarantees are paramount. A prominent example is Ethereum, where Keccak-256 is used extensively in transaction validation, block hashing, and smart contract execution.

In this thesis, Keccak-256 is included not because of raw speed but because of its relevance in production distributed systems, where it demonstrates the trade-off between cryptographic strength and computational efficiency.

2.2.3 BLAKE3

The BLAKE3 cryptographic hash function [13] is an evolution of the BLAKE2 cryptographic hash function [14], providing higher performance and introducing several additional features:

- Support for hashing, keyed hashing, and key derivation modes.
- No additional space cost for keyed hashing.
- Parallelizable output generation.

BLAKE3 employs a binary tree structure that splits the input into 1024-byte chunks, which are treated as the leaves of the tree. The final chunk may be shorter, but it cannot be empty (unless the entire input is empty). This design enables unlimited parallelism, as each chunk can be compressed independently, allowing efficient use of modern CPUs with SIMD instructions.

BLAKE3 achieves significantly better performance than both SHA-256 and SHA-512 on modern 64-bit architectures. Within the SHA family, SHA-512 generally outperforms SHA-256 on 64-bit machines [15].

BLAKE3's superior performance derives from its fundamentally different design philosophy. Unlike the inherently sequential SHA algorithms, its tree-based parallelism, fewer rounds, more efficient mixing function, and better cache locality enable it to outperform both SHA variants regardless of word size alignment considerations.

It provides a 128-bit security level and a 256-bit output.

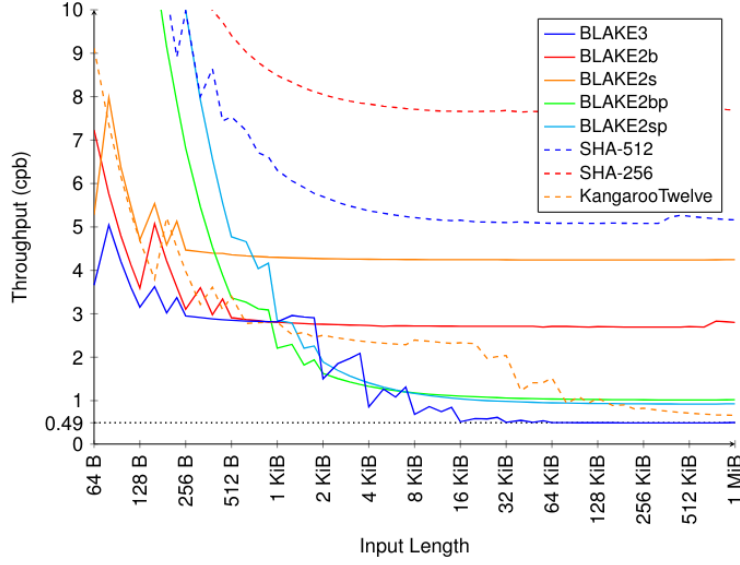


Figure 2.2: Single-threaded throughput of BLAKE3 and other hash functions on an AWS c5.metal instance, measured in cycles per byte (cpb). Lower values indicate fewer CPU cycles needed per byte.

Formally, for a message of length $n > 1024$ bytes, the left subtree covers a number of bytes equal to:

$$2^{10 + \lfloor \log_2 \left(\frac{n-1}{1024} \right) \rfloor}$$

The right subtree consists of the remainder. BLAKE3 supports input of any length $0 \leq \ell < 2^{64}$.

This section does not aim to describe the full BLAKE3 specification (e.g., its compression function or internal modes of operation), but rather to emphasize its practical performance benefits in the context of this work.

Performance

Figures 2.2 and 2.3 show benchmark results from an AWS c5.metal instance equipped with dual Intel Xeon Platinum 8275CL (Cascade Lake-SP) processors supporting AVX-512. These results highlight BLAKE3’s superior performance compared to other widely used hash functions.

In the context of this thesis, benchmarks were also conducted using the `mt-rs`¹ library to evaluate Merkle tree creation and proof generation under these three different cryptographic hash functions. For each function, three tests were performed

¹<https://crates.io/crates/mt-rs>

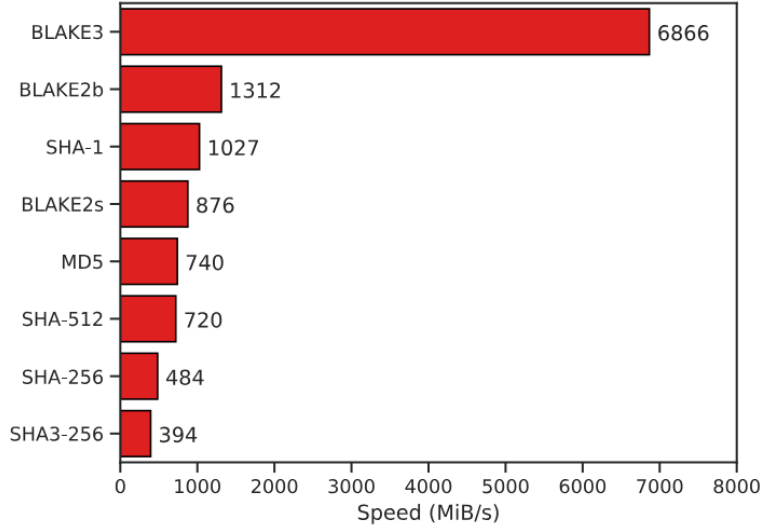


Figure 2.3: Hashing speed comparison of BLAKE3 and other hash functions on an AWS c5.metal instance with a 16 KiB input, using a single thread. Higher values (MiB/s) indicate faster processing.

with node data sizes of 5 MB, 10 MB and 15 MB. In each test, the benchmark measures the time required to construct the authentication path for a leaf, verify the corresponding root from that path, and repeat this process for all 10 nodes of the Merkle tree.

The results, reported in Table 2.1, demonstrate that BLAKE3 consistently outperforms both SHA-256 and Keccak-256 in terms of execution time.

Hash function	5 MB	10 MB	15 MB
SHA-256	89.901 ms	178.42 ms	268.53 ms
Keccak-256	521.49 ms	1.1334 s	1.3438 s
BLAKE3	73.091 ms	154.68 ms	219.79 ms

Table 2.1: Merkle tree benchmarks with 10 nodes per dataset size (5 MB, 10 MB, and 15 MB).

2.3 Consensus Protocols

This section provides background on the consensus protocols that were studied during the internship in order to evaluate how to integrate this Merkle-tree-based integrity verification protocol into a distributed setting. Although corruption de-

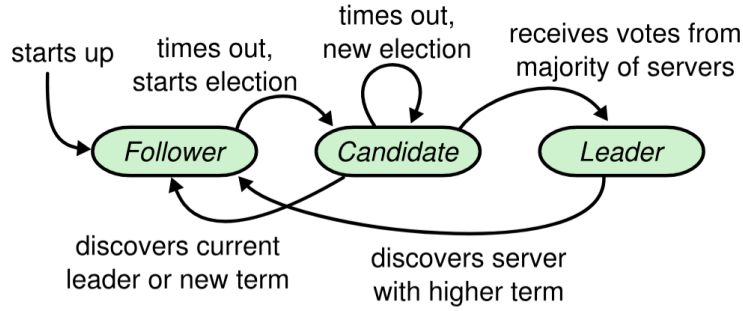


Figure 2.4: Server states. Followers only respond to requests from other servers. If a follower receives no communication, it becomes a candidate and initiates an election. A candidate that receives votes from a majority of the full cluster becomes the new leader. Leaders typically operate until they fail.

tection could be applied in a centralized environment using simple checksums, in a distributed cluster, a consensus algorithm is needed to coordinate nodes and ensure consistent state.

Several consensus mechanisms were examined, reflecting the long-standing debate between *leader-based* protocols (such as Raft, PBFT, and PB-Raft) and *leaderless* approaches (such as Flutter+Blink). Each design choice has implications for performance, fault tolerance, and implementation complexity.

2.3.1 Raft

Raft [16] is a consensus protocol designed to be understandable and practical, and it has become widely adopted in distributed systems such as `etcd` [17] and TiKV [18]. It tolerates *crash faults*, but not Byzantine behavior [19].

Each server on a Raft cluster is modelled as a finite state machine with three possible states:

- **Follower:** Passive state that responds to requests from the leader and candidates.
- **Candidate:** Initiates an election when a follower times out without hearing from a leader.
- **Leader:** Elected through majority vote, responsible for handling client requests and replicating logs.

In Figure 2.4, the three server states are illustrated using a finite state machine.

Leader election in Raft is randomized: followers start an election if they do not receive a heartbeat in a randomized timeout window (e.g., 150-300 ms). Candidates send **RequestVote** messages to all nodes, including their last log index and term, to ensure that outdated nodes cannot become leader. If a candidate obtains a majority of votes, it becomes the leader. Otherwise, it retries after another randomized timeout.

Once elected, the leader replicates client requests in the form of log entries using the **AppendEntries** message. Followers acknowledge receipt and once a majority confirms an entry, it is committed and applied to the state machines. This ensures safety (no two servers commit different values at the same log index) and availability (progress can be made as long as a majority of nodes are reachable).

Raft is crash fault-tolerant, but not Byzantine fault-tolerant. However, its simplicity and efficiency make it well-suited for small to medium-sized clusters.

2.3.2 Flutter+Blink

Flutter and Blink [20] are Byzantine fault-tolerant protocols that operate without a leader and without cryptographic signatures. They require at least $5f + 1$ servers to tolerate f Byzantine faults.

- **Blink:** Provides binary consensus using *Representative Binary Consensus (RBC)*, where a proposal is considered valid only if at least $f + 1$ correct servers support it. This in contrast to the single correct server required by Binary Consensus.
- **Flutter:** Builds on Blink to provide total-order broadcast, ensuring all servers agree on the same sequence of client messages. It achieves low latency with a best-case of $2\Delta + \epsilon$, where Δ is the network delay and ϵ is negligible.

Flutter uses a betting mechanism where clients attach timestamps (bets) to messages. Servers then order messages according to these bets, ensuring global consistency without requiring a centralized leader.

This makes Flutter+Blink interesting for highly adversarial settings, as they are leaderless, resilient to Byzantine behavior and even quantum-attack resistant (due to the absence of signatures). However, the $5f + 1$ replication requirement can be costly in practice.

2.3.3 Practical Byzantine Fault Tolerance (PBFT)

Practical Byzantine Fault Tolerance (PBFT), introduced by Castro and Liskov in 1999 [21], was the first protocol to show that Byzantine fault tolerance could be

practical in asynchronous environments. PBFT tolerates up to f Byzantine faults among $3f + 1$ replicas, using cryptographic signatures and message authentication codes (MACs) to prevent spoofing and replay attacks.

The protocol proceeds in three phases:

1. **Pre-prepare:** The leader proposes an order for client requests.
2. **Prepare:** Replicas exchange messages to confirm the proposal and ensure consistent ordering.
3. **Commit:** Replicas agree to execute the request once a quorum of matching prepare messages is observed.

A client considers its request successful once it receives $f + 1$ valid replies. If a timeout occurs, the request is retransmitted.

PBFT guarantees both safety (no two correct replicas decide differently) and liveness (progress is eventually made under partial synchrony). However, the communication overhead is high: the preparation and committing phases require $O(n^2)$ messages, limiting scalability.

Despite being somewhat outdated, PBFT remains foundational and continues to inspire more efficient Byzantine consensus protocols.

2.3.4 PB-Raft: A Byzantine Extension of Raft

Raft is widely used due to its simplicity and efficiency, but it only tolerates crash faults. PBFT tolerates Byzantine faults but at a high communication cost. PB-Raft [22] is a recent proposal that aims to combine the strengths of both.

Key features of PB-Raft include:

- **BLS signatures [23].** Allow short, aggregable multi-signatures that improve efficiency in log replication.
- **PageRank-inspired leader election.** Nodes are ranked by a probability score. Nodes with higher scores use shorter timeouts, balancing fairness and responsiveness.
- **Semi-synchronous model.** Assumes bounded network delays while tolerating Byzantine behavior.

Compared to PBFT, PB-Raft reduces message complexity by adopting Raft's two-phase replication approach while retaining Byzantine resilience.

2.3.5 Summary

In summary:

- **Raft** is practical, simple and widely adopted for crash fault tolerance.
- **Flutter+Blink** achieves leaderless, low-latency Byzantine consensus but requires many servers.
- **PBFT** provides strong Byzantine fault tolerance but at high communication cost.
- **PB-Raft** is a hybrid approach that adapts Raft for Byzantine environments.

For the scope of this thesis, Raft was chosen as the consensus algorithm due to its simplicity, maturity and suitability for a small cluster without Byzantine assumptions.

2.4 Reed-Solomon

This section provides background on Reed-Solomon coding to give the reader a clearer picture of Cubbit’s infrastructure and the context in which the proposed integrity verification mechanism was tested.

2.4.1 Classical Reed-Solomon coding

Reed-Solomon error correction [24] is one of the most widely used error correction codes, applied in digital communications, storage systems, and network protocols.

A Reed-Solomon code is defined over a finite field F_q , where F denotes the finite field and q is the size of its alphabet (typically a power of two, e.g. $q = 2^8$ for byte-oriented operations).

Classically, a Reed-Solomon code is parameterized by two values: the block length n , representing the total number of symbols in a codeword (data plus redundancy), and the message length k , representing the number of original data symbols, with $k < n \leq q$.

The encoder maps the k data symbols m_0, m_1, \dots, m_{k-1} to a polynomial of degree at most $k - 1$:

$$P(x) = m_0 + m_1x + m_2x^2 + \dots + m_{k-1}x^{k-1}. \quad (2.3)$$

This polynomial is evaluated at n distinct points x_1, x_2, \dots, x_n in F_q , producing n encoded symbols. The first k symbols correspond to the original data, while the remaining $n - k$ symbols are redundancy.

The key property of Reed-Solomon coding is that any subset of k symbols from the n encoded symbols is sufficient to reconstruct the original message using polynomial interpolation (e.g. Lagrange interpolation). This allows recovery even if some symbols are lost or corrupted.

2.4.2 Cubbit's adaptation

Cubbit employs Reed-Solomon coding to store files reliably across multiple nodes in its geo-distributed network. Unlike the classical definition, in Cubbit's implementation the total number of shards stored across the network is $n + k$, where n denotes the number of data shards and k the number of redundancy shards.

For example, with three nodes, a file could be split into three data shards, distributed one per node. If the system is configured with $k = 1$, only $n = 2$ shards are required to reconstruct the original file. Thus, even if one node is offline, the user can still recover the file successfully.

3 Architecture

This chapter describes the architecture of the proposed integrity verification protocol. First, the Rust library developed specifically for this project is introduced, designed to operate efficiently both at the folder level and on individual data items. Then, the organization of the Merkle tree within the system is discussed, including how the nodes (also referred to as *agents*) exchange information through the Raft cluster. Particular attention is given to scenarios in which some agents are temporarily unavailable (during uploads or during corruption checks) and how the system leverages the Raft log to maintain a consistent view of per-agent root hashes. This ensures that corruption verification can proceed safely and correctly, even when some agents lag behind or remain offline, independently of the Reed-Solomon requirement.

3.1 Merkle Tree Library

As discussed in Section 2.1, the integrity verification protocol relies fundamentally on the Merkle tree data structure. Despite the widespread use of Merkle trees in the literature and in applications such as blockchains, there are relatively few general-purpose and reusable libraries available online. This is largely because implementations are often developed *ad hoc*, tailored to the needs of a specific infrastructure or application domain.

To overcome this limitation, a dedicated library was developed in Rust¹, named `mt-rs`. The library is distributed under a BSD-3 Licence on Crates.io², with its source code publicly available at <https://github.com/boozec/mt>.

Hasher The construction of a Merkle tree begins with the definition of a *hasher*, i.e., the cryptographic hash function applied to the leaves and internal nodes of the tree. This enables direct experimentation with different trade-offs between performance and security. The design allows developers to implement custom

¹<https://www.rust-lang.org>

²<https://crates.io/crates/mt-rs>

hashers by instantiating the trait `Hasher`, which requires only the implementation of the `hash` method. Listing 1 illustrates a simple example of a user-defined hasher.

```
1 use mt_rs::hasher::Hasher;
2
3 pub struct FooHasher;
4
5 impl Hasher for FooHasher {
6     fn hash(&self, input: &[u8]) -> String {
7         let sum: u32 = input.iter().map(|&b| b as u32).sum();
8         format!("foo_{:x}", sum)
9     }
10 }
```

Listing 1: Example of a custom hasher `FooHasher`, which hashes an input as a string with the prefix "foo_" followed by the sum of the integer values of its bytes, in hexadecimal format.

The library provides three default hashers: `SHA256Hasher`, `Keccak256Hasher`, and `Blake3Hasher`. They correspond to the functions analyzed in Section 2.2.

Tree construction A Merkle tree is represented by the structure shown in Listing 2. It can be instantiated either from raw in-memory data using the `new` method or from the contents of files and folders using the `from_paths` method (Listing 3). This dual approach supports both synthetic testing and real-world scenarios, such as integrity verification of storage systems, by avoiding repeated disk reads.

```
1 pub struct MerkleTree {
2     /// Leaf nodes at the base of the tree
3     /// (may include a duplicate for even pairing).
4     leaves: Vec<Node>,
5     /// Height of the tree (number of levels including root).
6     height: usize,
7     /// Root node of the Merkle tree.
8     root: Node,
9 }
```

Listing 2: `MerkleTree` structure definition, where `Node` is an ad hoc structure that includes additional information and methods.

```

1  impl MerkleTree {
2      pub fn new<I, T, H>(hasher: H, data: I) -> Self
3      where
4          I: IntoIterator<Item = T>,
5          T: AsRef<[u8]>,
6          H: Hasher + 'static + std::marker::Sync,
7      { /* ... */ }
8
9      pub fn from_paths<H>(hasher: H, paths: Vec<String>) -> Self
10     where
11         H: Hasher + 'static + std::marker::Sync + Clone,
12     { /* ... */ }
13 }

```

Listing 3: Signatures of the `new` and `from_paths` methods. A concrete `Hasher` is always provided when defining a Merkle tree.

Internally, both methods translate the input data into leaf nodes of type `Node` and then invoke the builder function (Listing 4), which assembles the tree level by level. The construction algorithm ensures binary balance by duplicating the last node when the number of nodes is odd.

Parallelization is achieved through the `par_chunks` method of the Rayon crate³, which splits slices into disjoint chunks and computes parent nodes concurrently.

The tree is organized into *levels*: the leaves at Level 1, the root at the highest level, and internal nodes in between (Figure 3.1). This layered representation makes the structure conceptually simple. The root node is accessible through the `root()` method, and its hash can be retrieved directly. Unlike leaves and the root, internal nodes are not stored explicitly in the `MerkleTree` structure.

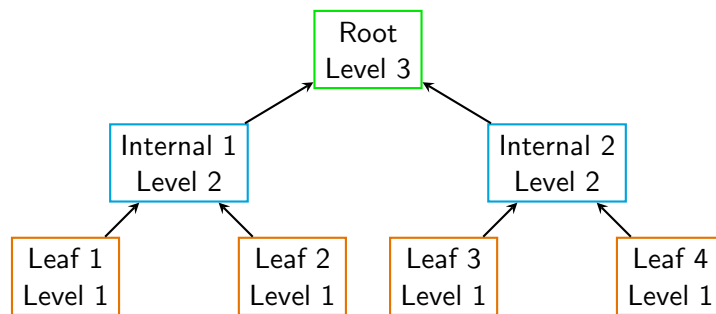


Figure 3.1: An example of a binary Merkle tree with 4 leaves, showing the different levels: leaves (Level 1), internal nodes (Level 2), and the root (Level 3).

³<https://crates.io/crates/rayon>

```

1  impl MerkleTree {
2      fn build<H>(hasher: H, mut leaves: Vec<Node>) -> Self
3      where
4          H: Hasher + 'static + std::marker::Sync,
5      {
6          let original_leaves = leaves.clone();
7          let mut height = 1;
8
9          while leaves.len() > 1 {
10             if leaves.len() % 2 != 0 {
11                 leaves.push(leaves.last().unwrap().clone());
12             }
13
14             leaves = leaves
15                 .par_chunks(2)
16                 .map(|pair| {
17                     let combined = [
18                         pair[0].hash().as_bytes(),
19                         pair[1].hash().as_bytes()
20                     ]
21                     .concat();
22
23                     let hash = hasher.hash(&combined);
24
25                     Node::new_internal(hash, pair[0].clone(), pair[1].clone())
26                 })
27                 .collect();
28
29             height += 1;
30         }
31
32         MerkleTree {
33             leaves: original_leaves,
34             height,
35             root: leaves.into_iter().next().expect("root not found"),
36         }
37     }
38
39 }

```

Listing 4: Build method for constructing the Merkle tree from the leaves upward. The `height` variable tracks the number of levels.

Listing 5 demonstrates printing the Merkle tree root hash. The `hash()` method of each node returns the computed hash as a string.

```

1 let data = &["hello".as_bytes(), "world".as_bytes()];
2 let tree = MerkleTree::new(Blake3Hasher::new(), data);
3 println!("Merkle root: {}", tree.root().hash());

```

Listing 5: Snippet of code that prints the Merkle root hash of a tree with two byte strings as leaves.

Proof generation and verification The library also supports Merkle proofs, which enable verification that a given leaf belongs to a specific Merkle tree. Proofs are generated and verified via implementations of the `Proofer` trait (Listing 6). A Merkle proof is expressed as sequences of `ProofNode` elements, which encode the sibling hashes encountered on the path from the leaf to the root. Users may define custom proofer if needed.

```

1 /// Represents a single step in a Merkle proof path.
2 pub struct ProofNode {
3     pub hash: String,
4     pub child_type: NodeChildType, // Left or Right
5 }
6
7 /// A Merkle proof containing the path from a leaf to the root.
8 pub struct MerkleProof {
9     pub path: Vec<ProofNode>,
10    pub leaf_index: usize,
11 }
12
13 pub trait Proofer {
14     /// Generates a Merkle proof for the data at the specified index
15     fn generate(&self, index: usize) -> Option<MerkleProof>;
16
17     /// Verifies that a piece of data exists in the tree using a Merkle proof
18     fn verify<T>(&self, proof: &MerkleProof, data: T, root_hash: &str) -> bool
19     where
20         T: AsRef<[u8]>;
21 }

```

Listing 6: The `Proofer` trait.

In this work, the `DefaultProofer` is used. Its implementation corresponds to proof generation (Algorithm 1) and proof verification (Algorithm 2). Unlike the `MerkleTree` structure, which does not store internal nodes, the `DefaultProofer` retains all levels.

Verification proceeds by iteratively reconstructing the root hash from the leaf

and its authentication path, comparing the result with the expected root. The implementation in Rust is reported in Listing 7.

```

1  impl<H> Proofer for DefaultProofer<H>
2  where
3      H: Hasher,
4  {
5      fn generate(&self, index: usize) -> Option<MerkleProof> {
6          if index >= self.levels[0].len() { return None; }
7          let mut path = Vec::new();
8          let mut current_index = index;
9          for level in &self.levels[..self.levels.len() - 1] {
10             let sibling_index = (current_index ^ 1).min(level.len() - 1);
11             let sibling = &level[sibling_index];
12             let child_type = if sibling_index < current_index {
13                 NodeChildType::Left
14             } else {
15                 NodeChildType::Right
16             };
17             path.push(ProofNode { hash: sibling.hash().to_string(), child_type });
18             current_index >>= 1;
19         }
20         Some(MerkleProof { path, leaf_index: index })
21     }
22
23     fn verify<T>(&self, proof: &MerkleProof, data: T, root_hash: &str) -> bool
24     where
25         T: AsRef<[u8]>,
26     {
27         let mut current_hash = self.hasher.hash(data.as_ref());
28         for proof_node in &proof.path {
29             let combined: String = match proof_node.child_type {
30                 NodeChildType::Left =>
31                     format!("{}", proof_node.hash, current_hash),
32                 NodeChildType::Right =>
33                     format!("{}", current_hash, proof_node.hash),
34             };
35             current_hash = self.hasher.hash(combined.as_bytes());
36         }
37         current_hash == root_hash
38     }
39 }

```

Listing 7: Implementation of the Proofer trait for DefaultProofer. The proof is built by traversing the tree levels and collecting sibling hashes along the path.

Example and Conclusion The complete workflow of the library is illustrated in Listing 8. In this test, a Merkle tree is constructed from the folder *pics*, which contains three files. The program verifies the basic properties of the tree, such as its height, and root hash, before generating a Merkle proof for the first leaf. Finally, the proof is successfully verified against the computed root hash, confirming the correctness of both tree construction and proofing. This example brings together the key components of the *mt-rs* library (hashers, tree building, and proof generation) and demonstrates their integration in practice, concluding the presentation of the Merkle tree library by showing how the system operates end-to-end on real data.

```

1  let hasher = Blake3Hasher::new();
2  let folders = vec![String::from("pics/")];
3
4  let tree =
5      MerkleTree::from_paths(hasher.clone(), folders);
6
7  assert_eq!(tree.height(), 3);
8  assert_eq!(
9      tree.root().hash(),
10     "a08c44656fb3f561619b8747a0d1dabe97126d9ed6e0cafb7ce08ebe12d55ca"
11 );
12
13 let proofer = DefaultProofer::new(
14     hasher.clone(),
15     // Recursively hashes the contents of files and directories.
16     hash_dir(hasher.clone(), folders),
17 );
18
19 let proof = proofer.generate(0).expect("proof generation failed");
20
21 assert!(proofer.verify(
22     &proof,
23     // Read the content of the first leaf read by the folder pics/
24     &fs::read("pics/photo0.png").expect("file not found"),
25     "a08c44656fb3f561619b8747a0d1dabe97126d9ed6e0cafb7ce08ebe12d55ca"
26 ));

```

Listing 8: End-to-end test of the *mt-rs* library: building a Merkle tree from the folder *pics* (with three files), checking its properties, and verifying that a proof for the first leaf matches the expected root hash.

3.2 File organization

This section describes how files are structured and managed within the proposed integrity verification protocol, highlighting the integration of Merkle trees with Cubbit’s existing Reed-Solomon-based infrastructure. As discussed in Section 2.4.2, each file is split into $n + k$ shards, with each shard distributed to a different agent (i.e., node).

To uniquely identify each file and its shards, the original filename is converted into a random lowercase hexadecimal string (e.g., `ff4c4b3`). Each shard is then appended with the identifier of the agent storing it (e.g., `ff4c4b3.1` for the shard on Agent 1), facilitating tracking and reconstruction.

When a user downloads a file, the system retrieves the shards from the respective agents and reconstructs the file using the Reed-Solomon algorithm. The reconstructed file is then returned to the user. In reality, the complete flow also involves encryption and decryption steps, but these are not relevant to understanding how files are organized for the purposes of this discussion.

As explained in Section 3.1, the developed Merkle tree library can operate directly on a list of folders. For this reason, the file organization within the proposed architecture can easily adopt a two-level folder hierarchy. For example, given a file named `ff4c4b3`, the file is stored under the path `ff/4c/4b3`. Another file, such as `ff4c61a`, is stored under the path `ff/4c/61a`, meaning that the folder `ff/4c` contains both files. This hierarchical organization is illustrated in Figure 3.2.

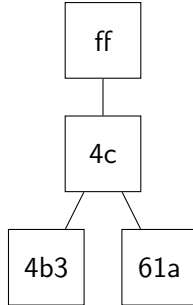


Figure 3.2: organization of files under the folder `ff`, represented as a tree structure.

From this figure, the reader can observe that `4c` can be regarded as an internal node with two leaves. For a larger example, Figure 3.3 shows how the same organization scales when more files are stored in the folder `ff`. At this scale, the overall structure resembles a larger tree with `ff` as the root.

It is important to clarify, however, that the diagrams so far represent *directory trees*, not Merkle trees. In a Merkle tree, internal nodes are not simply folders but cryptographic hashes computed from their children (the leaves or subtrees).

For this reason, the second-level folders in the figure cannot directly be considered internal nodes of a single Merkle tree. Instead, the entire filesystem should be viewed as a *Merkle tree forest*: each second-level folder forms an independent Merkle tree, while each top-level folder can itself be treated as a Merkle tree whose leaves are the root hashes of its subfolders.

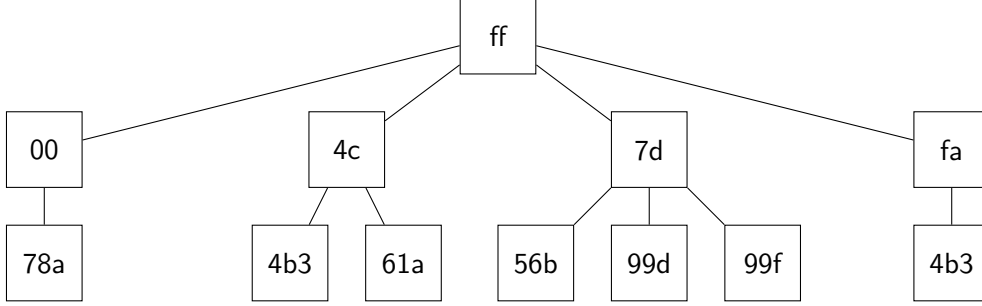


Figure 3.3: Extended example of file organization under **ff**, represented as a tree structure with multiple files.

If the leaves of a Merkle tree correspond to individual file blocks or shards, then a single root hash can represent the entire **ff** folder. Alternatively, smaller Merkle trees can be built independently for each subfolder. For instance, in Figure 3.3, one could compute four Merkle root hashes for the second-level folders and one root hash for the top-level folder **ff**.

This arrangement, referred to here as a *Merkle tree forest*, allows up to 256 top-level folders. Since only lowercase hexadecimal strings are used, ensuring compatibility with both case-sensitive and case-insensitive filesystems, the range spans from **00** to **ff**. Each top-level folder can contain up to 256 second-level folders, as the namespace is determined by four hexadecimal characters. Dividing the data into smaller trees is crucial for scalable and efficient verification, as will be detailed in the following section.

3.2.1 Storing different Merkle trees for each agent

Because each file is split into $n + k$ shards and distributed across different nodes, each agent maintains its own local file organization. As a result, there are effectively $n + k$ distinct filesystems, one for each agent. It should be noted that the sets of files stored by different agents may not be identical, since some agents may be offline during an upload. Nevertheless, the file is still successfully stored thanks to the Reed-Solomon requirements.

To better understand this, we can consider the entire filesystem of an agent as a tree structured as follows:

- **Root.** The global root, representing all files stored by the agent. In practice, this is rarely used because computing a Merkle tree for this element would require hashing the entire filesystem at once.
- **Second level.** The top-level folders (e.g., **ff**), each of which corresponds to the root of a Merkle tree for that folder.
- **Third level.** The second-level (or *sub*) folders (e.g., **ff/4c**), which are smaller Merkle trees containing only a subset of files.
- **Leaves.** The actual file data blocks.

The global root of the entire filesystem is avoided because it is too expensive to compute, especially across multiple agents that may be offline at any given time. At the other extreme, while each file could theoretically be validated individually, storing and checking a hash for every file would reduce the system to a simple checksum-based corruption detection scheme, which lacks scalability.

Instead, the system leverages intermediate Merkle trees at the *folder levels*. These allow integrity verification to be performed at different granularities: either locally within a subfolder or globally within a top-level folder, without the overhead of recalculating the root hash for the entire agent’s filesystem.

Figure 3.4 illustrates an example of this organization for a Reed-Solomon configuration with $n = 2, k = 1$. In this example, the top-level and second-level folders are highlighted with lighter and darker colors, respectively.

For each top-level folder, every agent computes and stores the Merkle root hash obtained from a Merkle tree whose leaves correspond to the *terminal files*. The same procedure is applied to second-level folders. For example, in Figure 3.4, Agent 1 computes and stores the Merkle root hashes of **fe**, **ff**, **fe/2d**, **ff/4c**, and **ff/6d**. Agents 2 and 3 follow the same procedure, maintaining the root hashes corresponding to their respective local filesystems.

A key property of these Merkle root hashes is that they can themselves be used as input for higher-level Merkle trees. The system computes aggregated Merkle trees from the folder roots and stores only the resulting root hashes in *string format*. This recursive organization is illustrated in Figures 3.5 and 3.6.

The distinction between top-level and second-level folder roots becomes largely irrelevant in storage terms: both are represented uniformly in a map, where the key is the folder identifier (two characters for a top-level folder, five for a second-level folder) and the value is the corresponding root hash. This raises a couple of questions: which component is responsible for storing and maintaining this map, and why does the system use two levels of folders instead of just one?

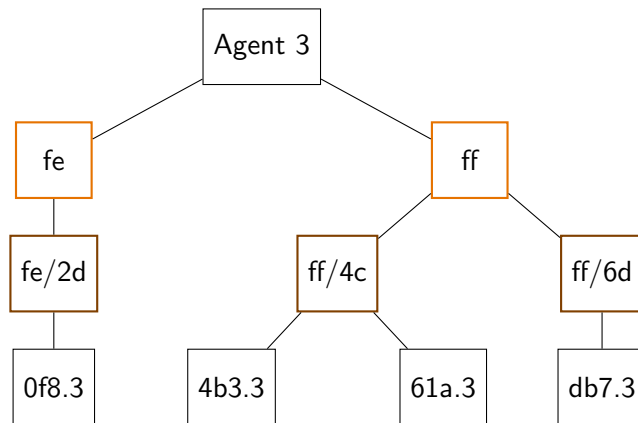
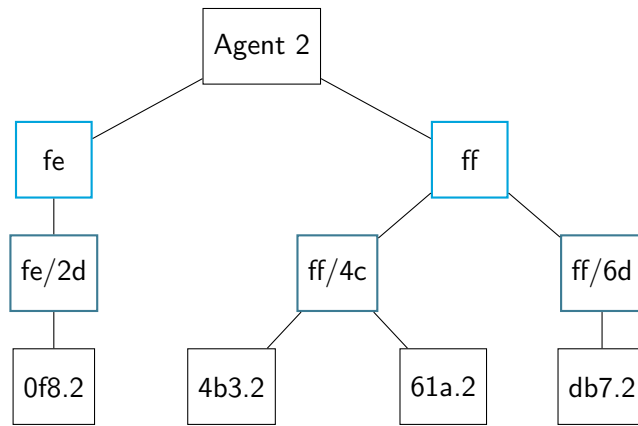
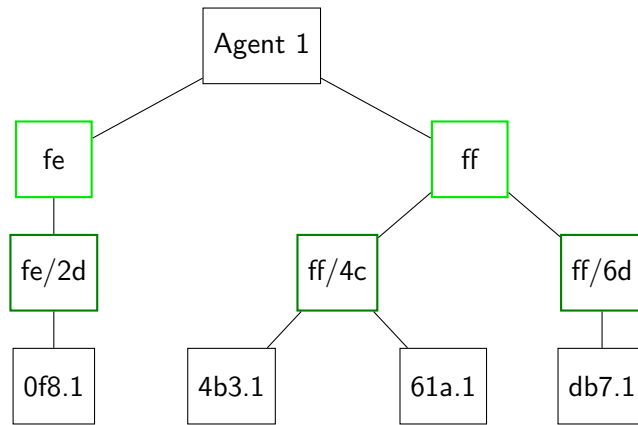


Figure 3.4: Example of filesystems for Agent 1, Agent 2, and Agent 3.

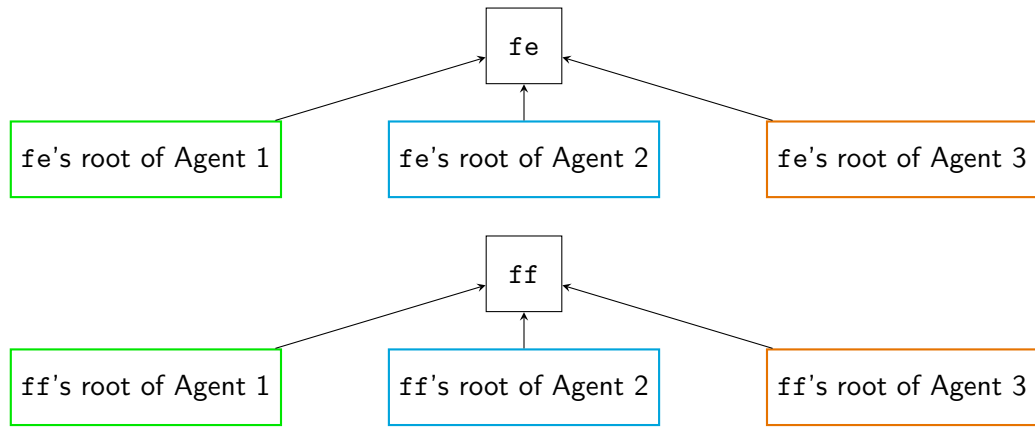


Figure 3.5: Merkle tree constructed from the root hashes of top-level folders. Each folder root acts as a leaf in this Merkle tree.

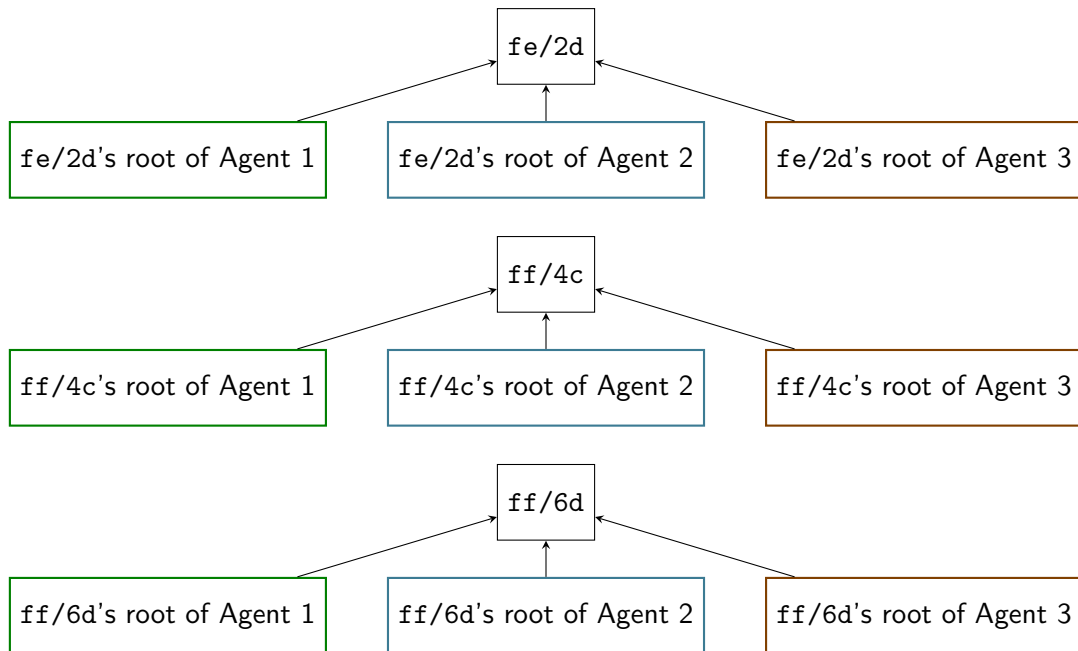


Figure 3.6: Merkle tree constructed from the root hashes of second-level folders. Each folder root acts as a leaf in this Merkle tree.

3.3 A Raft Cluster for File Uploads

In Section 2.3.1, the Raft consensus algorithm was introduced. This section explains its role within the proposed integrity verification protocol, focusing on how Raft enables global agreement among agents on the Merkle root hashes associated with different folders.

As discussed in the previous section, there is no practical distinction between top-level and second-level folder roots: both are stored uniformly. The key requirement is that each agent must be aware of the Merkle root hash of every folder *globally*, not just for its own local filesystem. This consistency is ensured through a Raft cluster, in which all agents act as nodes. Each node maintains a replicated log that functions as a command list of operations for a distributed key/value store, where folder identifiers serve as keys and the corresponding Merkle root hashes serve as values. Ideally, every correct node maintains an identical log, guaranteeing global agreement.

In practice, the Raft log is a sequence of messages broadcast by the leader to all nodes. Since the Raft cluster includes all agents, the terms *node* and *agent* can be used interchangeably. If an agent is online, it is part of the Raft cluster as well.

The log allows each agent to reconstruct *two levels* of a map, corresponding to the two levels of folder roots. Whenever a node restarts or rejoins the cluster, the log is replayed to restore state consistency. For example, in the scenarios illustrated in Figures 3.5 and 3.6, each agent would maintain a single map such as:

```
roots = {  
  # (1) Roots of top-level folders:  
  "fe":  "root hash of fe",  
  "ff":  "root hash of ff",  
  
  # (2) Roots of second-level folders:  
  "fe/2d": "root hash of fe/2d",  
  "ff/4c": "root hash of ff/4c",  
  "ff/6d": "root hash of ff/6d"  
}
```

Listing 9: Example of a map of Merkle root hashes. Whether the key represents a top-level or second-level folder is irrelevant for now.

Only the Raft leader is allowed to append new messages to the log. In other words, one designated agent is responsible for broadcasting updates so that all other agents converge on the same global map.

Figure 3.7 shows the sequence of events when a user uploads a file via the

gateway (the service exposed for uploads and downloads). The gateway (GW) communicates directly with all agents, and the agents form a Raft cluster. Each action triggers local computations, and the figure illustrates how updates propagate through the system:

- (1) The gateway receives a file, applies Reed-Solomon encoding, and splits it into $n + k$ shards. It generates a random salt (e.g., two bytes) and appends it to the filename (e.g., `photo.png24`). The salt prevents filename collisions and ensures randomized placement of the shards. Each shard is then sent to a different agent.
- (2) Each agent uses a deterministic algorithm to transform the filename+salt into a unique hexadecimal identifier (e.g., `ff4c4b3`). This ensures the file is placed in a folder not previously used or marked as corrupted. The file is then stored under a two-level folder hierarchy (e.g., `ff/4c/4b3`). Each agent appends its identifier (i.e., `.1`, `.2`, `.3`) and saves the shard locally (e.g., `ff/4c/4b3.1` for Agent 1).
- (3) Each agent computes the updated Merkle root hashes for the affected folders (e.g., `ff` and `ff/4c`) and sends them to the leader. Since any file modification propagates to the corresponding folder root, this step ensures consistency even when the top-level or second-level folders already contain files.
- (4) The leader aggregates the roots received from all agents and computes global Merkle roots for each folder as illustrated in Figures 3.5 and 3.6 (e.g., one for `ff`, one for `ff/4c`). The leader appends these values to the Raft log, which is replicated across the cluster.

As a result, all agents maintain an up-to-date map from folder names to their latest root hashes, as illustrated in Listing 9.

In contrast to the illustration in Figure 3.7, in practice the leader updates the global root hashes incrementally, immediately after each hash is received in step 3. Following the reception of the first update (3a), the leader computes the corresponding root values and appends them to the Raft log; the same process occurs after (3b) and again after (3c). Since Raft operates under a leader-based architecture, the exact order and timing of these messages is inconsequential: once all updates have been processed, all agents in the cluster will converge to an identical final state. This incremental propagation is crucial in scenarios involving partial uploads, which will be examined in the following sections.

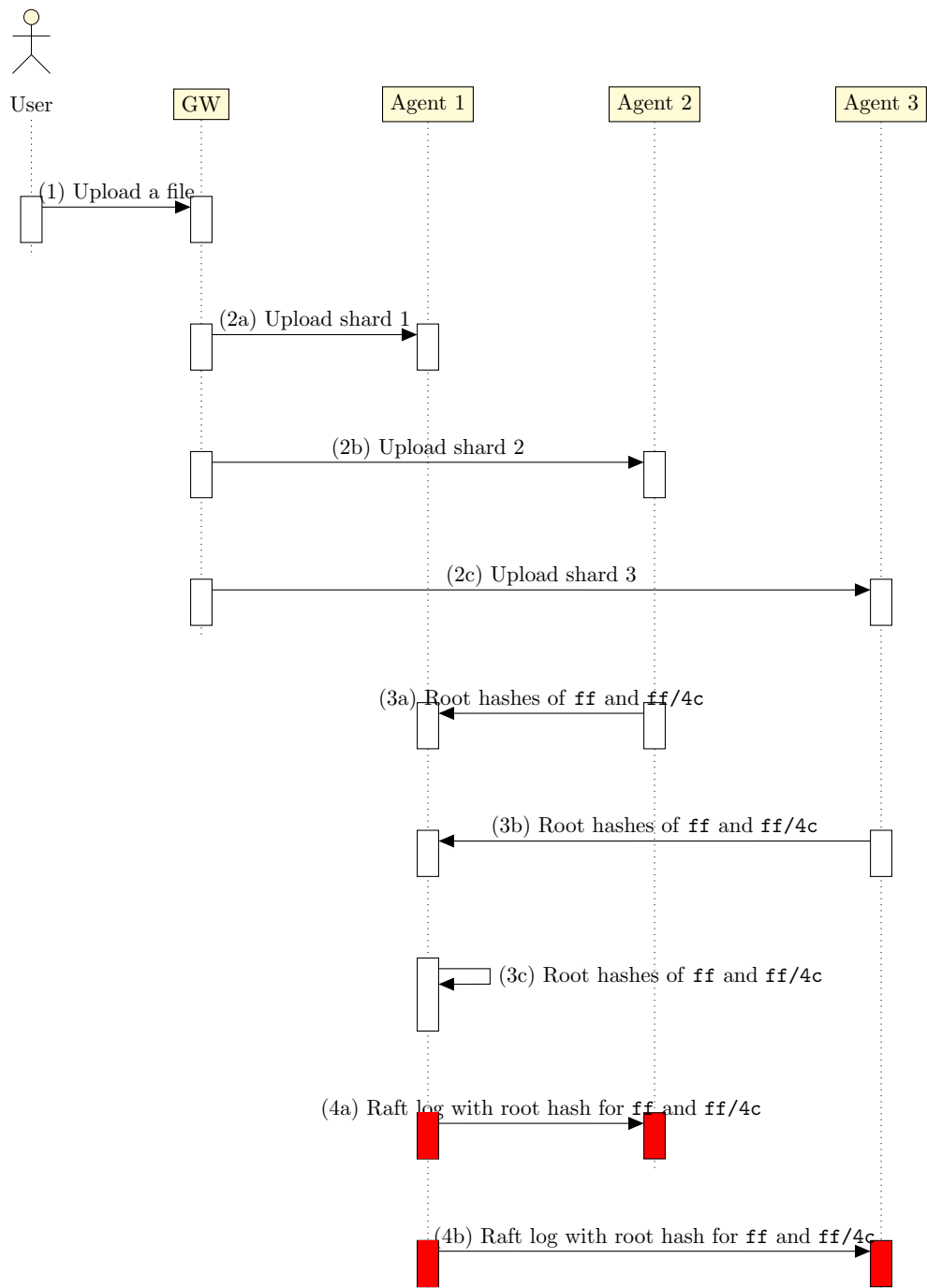


Figure 3.7: Sequence diagram for uploading a file. In this example, Agent 1 is the Raft leader and the uploaded file has a path starting with `ff/4c`.

3.3.1 Corruption Check

While Figure 3.7 illustrates how uploads are handled, an equally important question remains: how can the system detect corrupted files? This is the purpose of the *Corruption Check* process.

The process, executed at regular intervals for all top-level folders, is initiated by the leader. This responsibility lies with the leader because it is the only agent authorized to append new entries to the log. If corruption is detected, the leader records the result in the Raft log, thereby propagating the information consistently to all other agents.

Although earlier sections emphasized that top-level and second-level folders are stored uniformly, a practical distinction emerges during corruption checks. If a top-level folder is verified as intact, there is no need to check its subfolders. This follows from the Merkle tree property: any modification to a leaf propagates upward, changing the root. Thus, an unchanged top-level root implies that all second-level folders beneath it are also intact. Conversely, if a top-level folder's root does not match, the leader must recursively verify all second-level folders belonging to it.

In the best case, only the top-level folders need to be examined (a maximum of 256 keys, 16^2). In the worst case, when every top-level folder fails verification, all second-level folders must also be checked (up to 65536 keys, 16^4). This scenario corresponds to widespread corruption, where each top-level folder contains at least one corrupted file.

Figure 3.8 illustrates the process for a top-level folder:

- (1) The leader queries $n + k$ agents for the Merkle root hash of a given top-level folder (e.g., `ff`). It then applies the Merkle proof verification procedure, comparing the collected root hashes against the previously stored root (e.g., `roots["ff"]`).
- (2) The leader appends the result of this verification to the Raft log, broadcasting whether the folder is corrupted. If the folder is marked as corrupted, the process is recursively repeated for all of its second-level subfolders (e.g., `ff/4c` and `ff/6d`).

As a result, all agents share a consistent view of which folders are marked as corrupted. A top-level folder is corrupted if at least one of its subfolders is corrupted.

3.3.2 Corruption Check for Partial Uploads

The mechanisms described so far assumed that all agents are continuously online. In practice, temporary unavailability of agents is unavoidable. This subsection

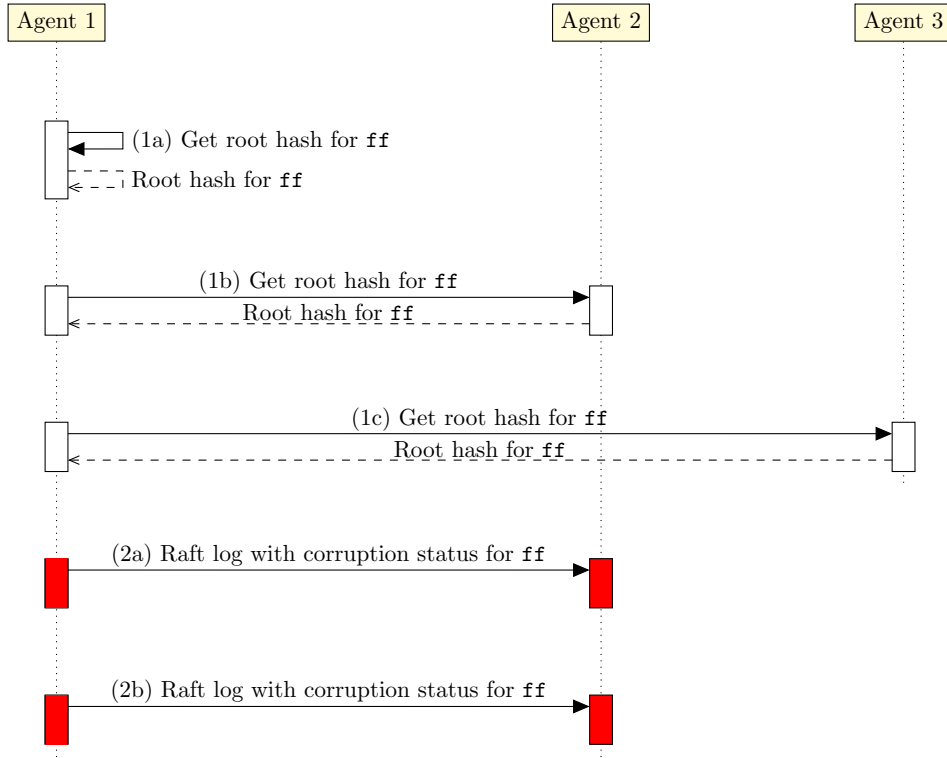


Figure 3.8: Sequence diagram illustrating the Corruption Check process for the top-level folder `ff`. Agent 1 is the Raft leader.

extends the model by considering two cases: (i) when an agent is offline during a file upload, and (ii) when one or more agents are offline during the corruption check itself.

To mitigate these cases, the data structures introduced in Listing 9 are extended. Instead of storing only a single Merkle root hash per folder (both top-level and second-level), the system also records Merkle root hashes for every agent. This results in two complementary maps:

- **roots:** a map from folder identifiers to global root hashes. Each value is the aggregated Merkle root computed over all agents' contributions for that folder.
- **agent_roots:** a map from folder identifiers to the set of per-agent root hashes. Each value explicitly tracks the current Merkle root hash for the corresponding folder, stored in an array indexed from 1 to $n + k$.

If an agent was offline during an upload, its entry in the array remains empty for a new entry or unedited for an older one. Thanks to the Raft log, these per-agent arrays are consistently replicated across all agents. This ensures that even if

a leader crashes and a new leader is elected, the Corruption Check phase remains unaffected.

An example is shown in Listing 10, where Agent 3 was offline during certain uploads. In this case, some entries of the `roots` map are computed using only two leaves, since the third leaf in the corresponding `agent_roots` entries is `nil`.

```
roots = {
  "fe": "root hash of fe",
  "ff": "root hash of ff",
  "fe/2d": "root hash of fe/2d",
  "ff/4c": "root hash of ff/4c",
  "ff/6d": "root hash of ff/6d"
}

agent_roots = {
  "fe": [
    "Agent 1 root hash of fe",
    "Agent 2 root hash of fe",
    "Agent 3 root hash of fe"
  ],
  "ff": ["Agent 1 root hash of ff", "Agent 2 root hash of ff", nil],
  "fe/2d": [
    "Agent 1 root hash of fe/2d",
    "Agent 2 root hash of fe/2d",
    "Agent 3 root hash of fe/2d"
  ],
  "ff/4c": ["Agent 1 root hash of ff/4c", "Agent 2 root hash of ff/4c", nil],
  "ff/6d": ["Agent 1 root hash of ff/6d", "Agent 2 root hash of ff/6d", nil]
}
```

Listing 10: Example of folder root hashes with $n = 2$, $k = 1$. Agent 3 was offline during the upload of files in `ff` folder.

It is important to note that root hashes are stored at the *folder* level, not per file. As a result, `agent_roots[<some_folder>]` may contain entries that are not perfectly aligned across agents. For example, Agents 1 and 2 may have already uploaded ten files into a folder, while Agent 3, having been offline, may only have one file in the same folder.

This apparent asymmetry does not compromise correctness. The reason is that `roots[<some_folder>]` is computed as a Merkle root over the entire array `agent_roots[<some_folder>]`. Even if one agent lags behind, the global root still represents a consistent snapshot of the folder state across all agents. During verification, the Merkle proof ensures that each agent's current hash (or stored historical hash, if offline) matches the position it contributed to in the global root.

Agent offline during upload If an agent is offline during an upload, the system can still guarantee correctness as long as the Reed-Solomon requirement is satisfied. In an $n + k$ configuration, at least n agents must be online, since n shards are sufficient to reconstruct the file on download.

If an agent was offline during an upload, its entry in the per-agent array remains empty (or unedited). Thanks to the Raft log, these arrays are consistently replicated across all agents. Because the system does not modify the entry corresponding to the offline agent, the Merkle root computed in `roots` correctly reflects the full folder state, including the filesystem status of the offline agent. Therefore, the global Merkle root remains consistent even if some agents are temporarily unavailable.

When the offline agent later rejoins, it synchronizes its metadata by replaying the Raft log. However, it does not automatically reconstruct the shards it missed during downtime. During a corruption check, the leader queries the folder root hashes from all agents. For an agent that was previously offline, the stored value in `agent_roots` is exactly what the leader expects. Thus, the check does not fail: the Merkle root returned by the previously offline agent is consistent with the snapshot that the leader uses for verification, assuming no corruption has occurred.

This reasoning naturally generalizes to the case where up to k agents are offline at the same time: as long as at least n agents remain available, the system continues to satisfy the Reed-Solomon requirement.

Agents offline during corruption check A more challenging scenario arises when some agents are offline during the corruption check itself. The set of agents currently online may differ from those that participated in the original upload. If the leader cannot collect the current Merkle root for a folder from all agents (even when some entries in `agent_roots` are `nil`) the corruption check for that folder must rely on the available data. Consequently, the check process is adapted to handle offline agents gracefully.

During a corruption check for a folder, the leader iterates over all $n+k$ positions:

- If agent i is online, it requests the current root hash from that agent.
- If agent i is offline, it retrieves the saved value from the corresponding slot in `agent_roots`.

Once all $n + k$ values are collected, the leader performs the Merkle proof verification against the global root hash stored in `roots`. This process is illustrated in Figure 3.9.

Returning to the example: suppose Agent 2 goes offline while Agent 3 comes online. During the corruption check of folder `ff`, the system uses the stored value of Agent 2's root from `agent_roots["ff"][2]`, while requesting a fresh root from

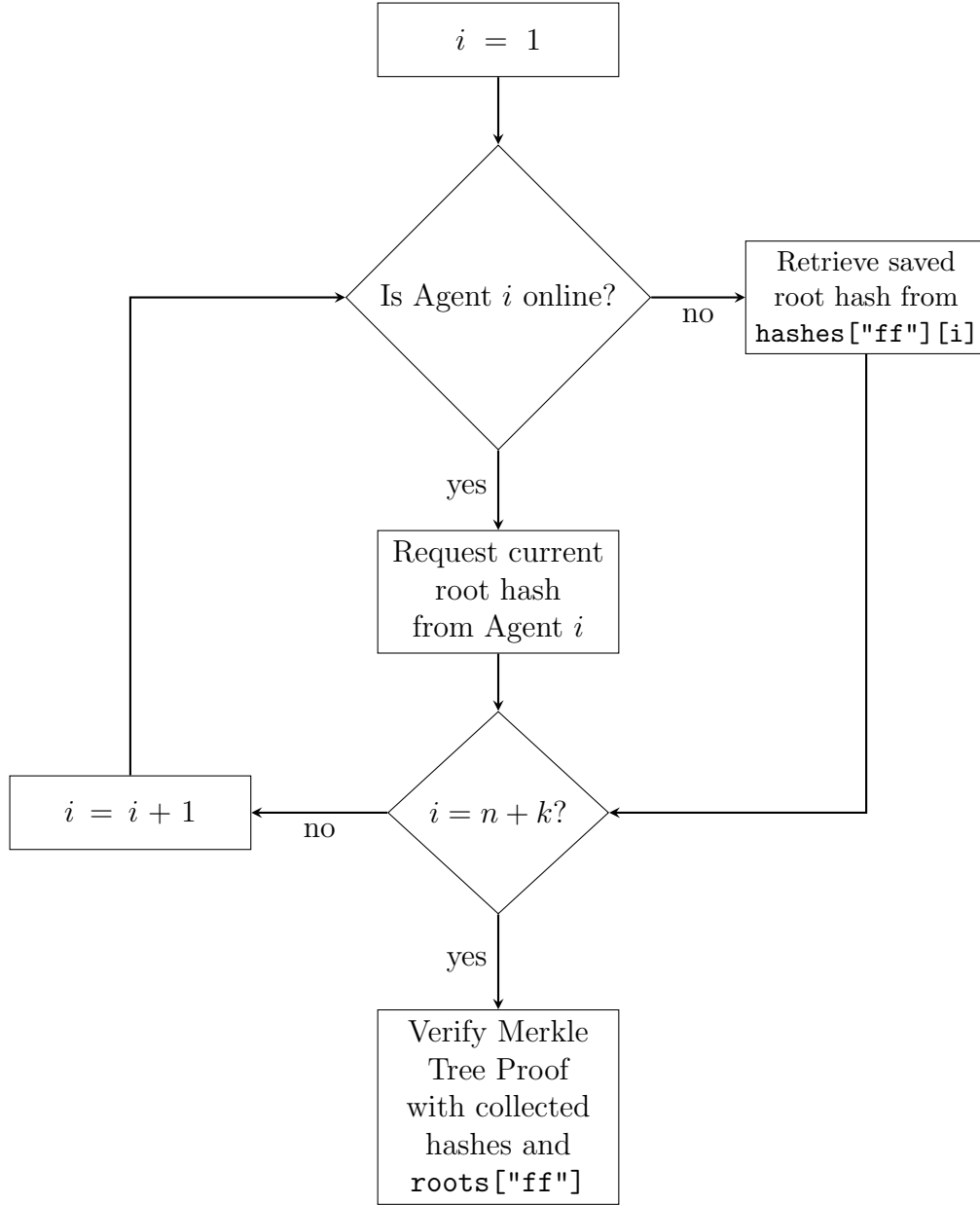


Figure 3.9: Corruption check process for the top-level folder **ff**, considering some agents may be offline.

Agent 3. If the Merkle proof verification succeeds, this guarantees that all currently online agents are consistent and uncorrupted. In this case, the status of offline agents is irrelevant:

- If the proof holds, online agents have uncorrupted data.
- If the proof fails, at least one online agent is corrupted, and the outcome is marked as a corruption regardless of the offline agents.

This highlights an important distinction: the Corruption Check 3.3.1 phase itself does not rely on the Reed-Solomon requirement of having n correct shards. Instead, it depends only on the fact that the Raft log ensures a consistent view of the per-agent root hashes across all agents. Offline agents may lag behind in state (or even remain offline for the entire process) without affecting the verification. In fact, it would be possible to perform the corruption check even if more than k agents are offline. The correctness of the two cases considered (Agents offline during upload and Agents offline during the corruption check) is ensured because the first case already satisfies the Reed-Solomon reconstruction requirement, while the verification itself relies solely on the consistency guaranteed by Raft. Therefore, the corruption check can safely verify the folder state based on the available information, independently of the offline agents.

3.3.3 Recovery of Missing Shards

In the previous subsection, the reader learned what happens when an agent is offline during a file upload. This subsection discusses how missing shards are reconstructed when a previously offline agent comes back online.

The sequence diagram illustrated in Figure 3.7 is simplified: every time a new shard is uploaded, the agent sends an acknowledgment to the leader. This allows the leader to maintain an up-to-date view of the cluster, tracking which agents are online and which have stored a shard for a given file, avoiding active pings or status checks. The acknowledgment is asynchronous, so the leader does not block waiting for responses. Meanwhile, the user receives confirmation through the gateway (GW), which handles shard uploads synchronously. In other words, shard storage and acknowledgment to the leader are independent processes.

Thanks to Raft, the leader keeps a log of all received acknowledgments. Recording this information in the Raft log ensures that every node in the cluster knows which agents were offline during the upload of a file.

During the download process, some previously online agents might now be offline, and vice versa. Even if the set of online agents at upload time satisfied the Reed-Solomon requirement, there is no guarantee that the currently online agents

hold enough shards (at least n) to reconstruct the file. When this happens, a recovery phase is necessary to restore the missing shards to ensure reconstruction.

Similar to the Corruption Check phase, a Recovery phase can be triggered to deliver missing shards to previously offline agents. The leader coordinates this process. To maintain consistency, the receiving agent recalculates the Merkle roots for both the top-level and second-level folders affected by the newly received shard. It then sends the updated roots back to the leader, which updates the corresponding i -th entries in `agent_roots` and recomputes the global `roots` for the folders. Once the missing shard is successfully restored, the leader records the update in the Raft log to notify all nodes that the shard has been sent and the new values for the relevant `roots` and `agent_roots` maps have been established.

Retaking the previous example shown in Listing 10, after a full recovery all entries in `agent_roots` are filled, as illustrated in Listing 11.

```
roots = {
  "fe":  "new root hash of fe",
  "ff":  "new root hash of ff",
  "fe/2d": "new root hash of fe/2d",
  "ff/4c": "new root hash of ff/4c",
  "ff/6d": "new root hash of ff/6d"
}

agent_roots = {
  "fe":  [
    "Agent 1 root hash of fe",
    "Agent 2 root hash of fe",
    "Agent 3 root hash of fe"
  ],
  # [...]
  "ff/6d": [
    "Agent 1 root hash of ff/6d",
    "Agent 2 root hash of ff/6d",
    "Agent 3 root hash of ff/6d"
  ],
}
```

Listing 11: Example of folder root hashes with $n = 2$, $k = 1$ after every agent received all the shards.

This chapter described how the Merkle tree solution was designed and integrated with a Raft cluster, explaining step by step how the main issues were addressed. The next chapter focuses on the implementation, presenting the developed solution and evaluating it through system-wide testing.

4 Implementation and Tests

This chapter provides a practical overview of the proposed integrity verification protocol by presenting a real implementation developed specifically for this work. The implementation consists of a standalone binary application built around the `mt-rs` library, employing the BLAKE3 cryptographic hash function, the Raft consensus algorithm, and the Reed-Solomon coding.

Rather than including extensive code listings, which would not significantly contribute to the goals of this thesis, the discussion highlights selected code snippets that illustrate how the individual components operate together in a coherent system. Finally, the chapter presents a series of benchmarks designed to evaluate the behavior of the implementation under various scenarios, such as node failures, varying numbers of agents, and datasets of different sizes and file counts.

4.1 Files in a Raft Cluster

As discussed in Section 3.3, the system is built upon a Raft cluster integrated with a storage mechanism based on Reed-Solomon coding. To study this integration, a Go¹ application was implemented, reconstructing a Cubbit-like infrastructure by layering a Raft cluster on top of Reed-Solomon redundancy. Go was chosen for its gentle learning curve and widespread adoption, including by companies such as Cubbit. Following the common project layout recommended for Go[25] all the developed services are organized within a single module. This structure avoids redundancy, such as duplicating the service message definitions described later. Each service is maintained separately as a distinct binary under the `cmd` folder, in accordance with Go best practices.

To investigate the communication patterns between the system components, two service APIs were implemented: a REST API, commonly used for web services, and a gRPC², developed by Google and based on Protocol Buffers (Protobuf), which allows precise definition of the message types transmitted over the network.

¹<https://go.dev/>

²<https://grpc.io/>

Listing A.1 illustrates the Protobuf definitions used by the agents, including messages for both gateway-agent and agent-agent interactions.

The distinctive feature of gRPC is that the Protobuf file can be directly compiled into Go code using a simple CLI, as shown in Listing 12.

```
protoc --go_out=. \
      --go_opt=paths=source_relative \
      --go-grpc_out=. \
      --go-grpc_opt=paths=source_relative \
      agent.proto
```

Listing 12: Protobuf compiler command that generates Go code from the service definition located at `agent.proto`.

This command generates two Go files:

- `agent.pb.go`, which contains the standard Protobuf message definitions and serialization code.
- `agent_grpc.pb.go`, which contains the gRPC client and server stubs necessary to implement the service endpoints in Go. The methods defined in Listing A.1 are represented as an interface in this file, and they must be implemented to enable communication between a gateway and the agent service, or among agents themselves.

Together, these files constitute the foundation for both gateway-to-agent and inter-agent communication in the system.

4.1.1 Gateway service

The Gateway service acts as the entry point for the user, as illustrated in step 1 of Figure 3.7. It is exposed via a REST API and manages file uploads and downloads by splitting files into $n + k$ shards using the Reed-Solomon algorithm and distributing them across the agents. The REST interface is intentionally minimal in this prototype, offering only two endpoints: one for uploading and one for downloading files. The upload endpoint requires the local file path and the desired filename, while the download endpoint requires only the filename.

Go provides a straightforward mechanism to instantiate a web server, as shown in Listing 13. The `mux` server maps REST paths to functions, referred to as handlers.

```

1 mux := &http.ServeMux{}
2 mux.HandleFunc("/upload", UploadHandler)
3 mux.HandleFunc("/download/{filename}", DownloadHandler)
4 http.ListenAndServe("<url>", mux);

```

Listing 13: Instantiation of a simple web server in Go.

Upload handler A partial implementation of the upload handler is shown in Listing A.2.

Some clarifications on the code in Listing A.2 are in order. The details of file encryption are omitted, since they are not central to the current discussion. Similarly, the internal implementation of Reed-Solomon encoding is abstracted: the key point is that the function `reedSolomon.Create` returns the $n + k$ shards from the encrypted file. Error handling is also simplified for readability, and the specific contents of the `jsonResponse` are not reported, as they are not relevant to the design.

The critical part lies in lines 14-16, where the `SendShard` method from the custom `rpc` module is invoked. This method serves as a wrapper around the generated gRPC client code contained in `agent_grpc.pb.go`. Its role is to establish the connection, transmit the shard, and delegate the call to the gRPC stub. The implementation of this wrapper is presented in Listing A.3.

However, this implementation alone is not sufficient. A corresponding gRPC server must also be defined to handle the data transmitted in lines 27-31. As explained earlier, the code in `agent_grpc.pb.go` only provides the interface definition; the concrete server-side logic needs to be implemented in order to process the incoming shard data. This aspect will be discussed in detail in the next section.

Download handler Equally important, though similar in structure to the previously presented `UploadHandler`, is the `DownloadHandler`. While not strictly necessary for system testing, it is useful in both real-world scenarios and tests, for example to verify that a downloaded file is not corrupted. A partial implementation is shown in Listing A.4.

As with the `UploadHandler`, certain implementation details are omitted for simplicity, such as how the correct salt is determined for each file and the internal workings of the Reed-Solomon reconstruction algorithm. The `rpc.GetAllShards` function serves as a wrapper, analogous to `SendShard` in Listing A.3. Internally, it executes gRPC calls to the `GetShard` method defined in the Protobuf file (Listing A.1). The server-side handling will be discussed in the following section.

4.1.2 Agent service

Each agent is responsible for storing its assigned shards locally and participates as a node in the Raft cluster. The total number of agents corresponds to the Reed-Solomon configuration $n + k$. Communication between the gateway and agents is implemented using gRPC, which enables efficient binary data transfer and supports a wide range of commands. Inter-agent communication also relies on gRPC, providing operations such as shard acknowledgments, cluster membership management, and retrieval of the current Merkle root hash for a given folder.

Instance new agent The Agent service must instantiate a new gRPC server at startup, while also initializing its participation in the Raft cluster. When a node starts a new cluster, the process is referred to as *bootstrapping*. A simplified version of the Agent service startup is shown in Listing A.5.

Some details are omitted in Listing A.5, such as error handling, but two elements are particularly important: the `Server` struct, which implements the service interface generated from the Protobuf definition, and the `newRaft` function, which initializes a new Raft instance.

For this prototype, the HashiCorp Raft implementation³ has been adopted. A partial implementation of `newRaft` is shown in Listing A.6.

Here, the `id` field identifies the node (e.g., `nodeA`), while `raftAddress` specifies the address where the Raft instance listens (e.g., `0.0.0.0:4001`). This address is distinct from the one used by the gRPC server.

Several components in Listing A.6 deserve further attention. The `logs` store persists the sequence of Raft log entries, ensuring that all operations proposed to the cluster are durable. The `stable` store maintains critical metadata, such as the current term and cluster configuration, which must survive restarts. The `snaps` store provides periodic snapshots of the state machine, enabling log compaction and preventing unbounded growth. Finally, the `fsm` represents the finite state machine, which applies committed log entries to the storage layer, managing shard placement and retrieval.

Together, these components enable each agent to participate reliably in the Raft consensus protocol, preserving consistency and fault tolerance across the distributed system.

The reader may notice that the cluster is bootstrapped only within the `if` statement in lines 24-33 of Listing A.6. The `bootstrap` flag is passed when calling `newRaft` at startup. Importantly, only one node per cluster performs the bootstrap step during initialization. All other agents must join the cluster by sending a `JoinRaft` request over gRPC, as illustrated in Listing A.7.

³<https://github.com/hashicorp/raft>

Meanwhile, the bootstrap node must handle these incoming gRPC requests, which is possible because every Raft node is also an agent, as shown in Listing A.8. As always, some details are omitted to have simpler snippets, such as the various error handling.

Handlers for upload and download The two gRPC calls `SendShard` and `GetShard`, introduced in Listings A.3 and A.4, are handled by the agents' gRPC servers, as illustrated in Listings A.9 and A.10. For simplicity, error handling and some path resolution details are omitted.

The key aspect to note is the inner go-function in Listing A.9, lines 9-28. This function retrieves the top-level and second-level folder roots for the shard. Differently than Figure 3.7, it then prepares a single gRPC request containing both roots (concatenated; each root is 32 bytes) and sends it to the leader. If the sender itself is the leader, the message is processed locally.

Command structure As introduced in Section 3.3.3, agents send acknowledgments to confirm that a shard has been successfully stored during a file upload. This mechanism can also be observed in the `SendShard` function in Listing A.9, lines 24 and 26.

Before presenting the server-side implementation of the `AckShard` call, it is necessary to clarify how messages are applied to the Raft log. This is achieved through a command-style object, consisting of an operation code (a simple integer) and an action value (an `interface{}` in Go). The Raft log interprets entries by first examining the operation code and then processing the corresponding action value. The definition is shown in Listing A.11.

The action value can then be extracted with a cast to a concrete type and dispatched using a `switch` statement on instance's `Code`.

Acknowledgment For simplicity, some details on the handling of the `AckShard` call on the server-side are omitted, including error handling and the explicit check that the current node processing the request is indeed the cluster leader. The server-side implementation is shown in Listing A.12, while Listing A.13 illustrates how new messages are applied to the Raft log.

The function `shardAcknowledge` updates the acknowledgment status for a given shard using a boolean array, where the i -th position corresponds to Agent i . Updates are applied with a bitwise-or (`done[i] || prevDone[i]`) and protected with a mutex to prevent race conditions during concurrent `r.Apply` calls.

The functions `saveRoot` and `saveAgentHash` persist Merkle roots and per-agent roots, respectively, as shown in Listing A.13. Unlike in previous sections, the two folder levels are split into four global maps (`roots1`, `roots2`, `hashes1`,

`hashes2`), which simplifies extensions to deeper folder hierarchies while also improving efficiency.

Each command action is associated with a concrete type such as `ShardDone`, `MerkletreeRootHash`, or `MerkletreeHash`. This design choice makes it easier to parse and interpret actions later on. Since Raft log messages are stored as raw bytes, serializing them into structured types provides a reliable way to access and manipulate individual parameters.

Finally, the `merkletree.RootHash` function, used to compute folder roots, will be discussed in detail in the following paragraph.

Compute Merkle trees As seen in the previous paragraph, there is a call to `merkletree.RootHash`, which takes as input an array of per-agent hashes of a top-level or second-level folder. Similarly, the reader may also have noticed a call to `merkletree.FolderRootHash`, which instead takes an entire top-level or second-level folder as input. These two usages appear in Listings A.12 and A.9, respectively.

At first glance, one might assume that these calls are directly invoking the Rust Merkle tree library. However, as explained in Section 3.1, the Merkle tree was implemented as a library in Rust, not as a standalone binary. To make it usable from the Go-based system, a dedicated binary was developed in Rust, wrapping the library functionality and exposing simple command-line options for root hash generation and proof verification. The flow is illustrated in Figure 4.1.

A partial implementation of this Rust binary is shown in Listing A.14. Depending on the flag `--file`, the binary constructs a Merkle tree either from a set of files or from raw data provided as arguments. For instance, after compiling and installing the binary as `mt-rs-bin`, the command `mt-rs-bin --file ff` computes the Merkle root hash for the folder `ff`, which corresponds to the use case in Listing A.9. Alternatively, aggregating per-agent root hashes allows commands such as `mt-rs-bin hash1-ff hash2-ff hash3-ff` to compute the global root hash for folder `ff`, as required in Listing A.12. In both cases, the binary produces only the Merkle root hash as a string, which the Go application captures and stores.

The binary can be extended with additional modes, such as proof verification. In this case, passing a `--proof` flag triggers Merkle proof validation instead of tree creation, as shown in Listing A.15. The output in this case is a boolean value (`true` or `false`) indicating whether the proof is valid.

For completeness, the Go module `merkletree` provides methods for proof verification and root computation; their prototypes are in Listing A.16. These are thin wrappers that internally call the Rust binary via `exec.Command` and capture its output. This design avoids the need for complex Go-Rust bindings, while taking advantage of the high-performance Rust implementation of the Merkle tree

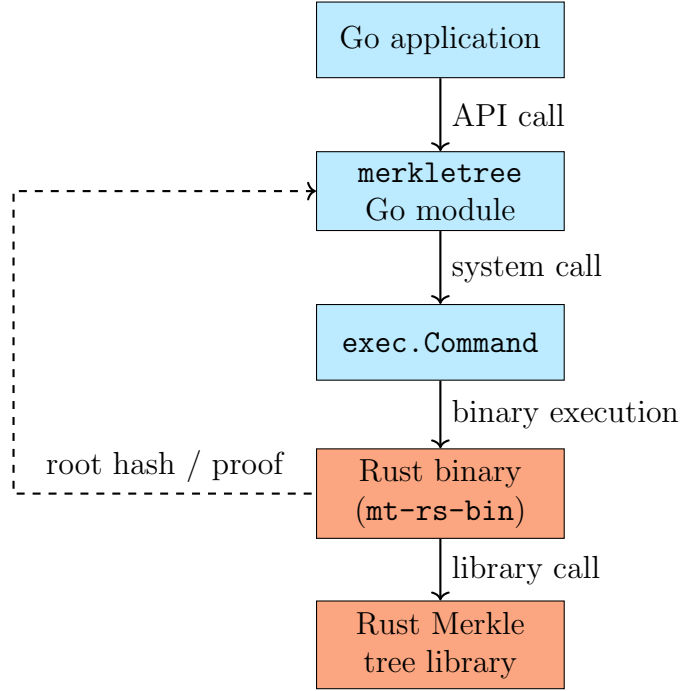


Figure 4.1: Interaction between Go and Rust components. The Go `merkletree` module invokes the Rust binary via `exec.Command`, which delegates computation to the Rust Merkle tree library.

library. In this way, the performance-critical logic remains in Rust, whereas the Go application retains a clean and simple interface for Merkle tree operations.

Signal corruptions Finally, this paragraph illustrates how the leader signals data corruption for a folder to the other agents in the Raft cluster. In Listing A.11, the reader has already seen the command code `SignalCorruption`, which is used here as the operation code. The associated action is defined by a folder name (top-level or second-level) and a boolean `CorruptionStatus` flag.

When the Corruption Check phase (Section 3.3.1) is triggered, the leader follows the sequence shown in Figure 3.8, while also respecting the flow for handling offline agents as illustrated in Figure 3.9.

A partial implementation of this flow is presented in Listing A.17. The global maps `hashes1` and `hashes2` store folder names as keys and per-agent hashes as values, and can be used as a backup if some agents are offline. If the first retrieved `data` for a top-level folder does not verify against its Merkle proof, the algorithm iteratively checks each second-level folder nested within it. The function `merkletree.IsPathCorrupted` builds a Merkle proof from the provided `data` and compares the computed root hash with the reference root. Internally, it in-

vokes the `mt-rs-bin` binary, as explained in the previous paragraph.

Consistency is ensured by Raft: the function `saveCorruptionState` updates a global `corruptions` map that associates each folder (independently of its level) with a boolean value. Since every update is persisted in the Raft log, each node in the cluster can rebuild the map locally and remain synchronized with the cluster state.

4.2 Testing Environment and Results

The previous section described how the system was implemented and how each component interacts within the complete flow, from a user that uploads a file to the leader performing the Corruption Check phase (showed in Section 3.3.1).

This section presents the testing environment, the scenarios used during evaluation, and the obtained results. The tests were executed on a cluster of nine machines running Ubuntu 24.04.1 LTS (GNU/Linux 6.8.0-51-generic x86_64). The specifications of the virtual machines are summarized in Table 4.1. The nodes were geographically distributed across the European continent.

Node ID	IPv4	Country	CPU(s)	RAM	Disk
GW	51.15.221.121	France	8	32 GB	45 GB
Agent 1	212.47.241.22	France	4	16 GB	45 GB
Agent 2	51.15.138.169	France	4	16 GB	45 GB
Agent 3	51.159.178.75	France	4	8 GB	45 GB
Agent 4	51.158.75.32	France	4	8 GB	45 GB
Agent 5	51.158.233.202	Netherlands	4	8 GB	45 GB
Agent 6	51.15.108.2	Netherlands	4	8 GB	45 GB
Agent 7	151.115.42.176	Poland	4	8 GB	45 GB
Agent 8	151.115.104.48	Poland	4	8 GB	45 GB

Table 4.1: Specifications of the machines used in the testing environment.

Each test scenario considered four parameters:

- **Number of agents:** total number of agents participating in the Reed-Solomon configuration of $n + k$ nodes.
- **Number of offline agents:** number of agents intentionally disconnected during the corruption check.
- **Number of files:** number of files included in the test.
- **File size:** size of each uploaded file. In the first four tests, each file is divided into $n + k$ shards, so the size of a single shard equals $\frac{\text{file size}}{\text{number of agents}}$.

All scenarios consider that some agents, respecting the Reed-Solomon requirement, could be offline during the uploads. In these scenarios, the time required for shard recovery, as described in Section 3.3.3, is included in the measurement. The corruption check procedure begins only after all shards have been successfully uploaded to the cluster. The total elapsed time, measured in seconds, is recorded from the initiation of the corruption check until its completion. A test is considered valid only if the system successfully detects any data corruption. Each plotted value represents the average total elapsed time over three independent runs.

Test 1: Large files, all agents online In the first scenario, 100 files of 100 MB each were uploaded, yielding a total dataset of 10 GB. Each file was divided into $n + k$ shards and distributed across the agents in the cluster. All agents remained online during the corruption check. Figure 4.2 shows the elapsed time for the corruption check as the number of agents increases from 3 to 8. As expected, the elapsed time increases with the number of agents, primarily due to additional network communication, coordination, and data verification overhead. The elapsed time ranges from 1.373 seconds with 3 agents to 23.892 seconds with 8 agents.

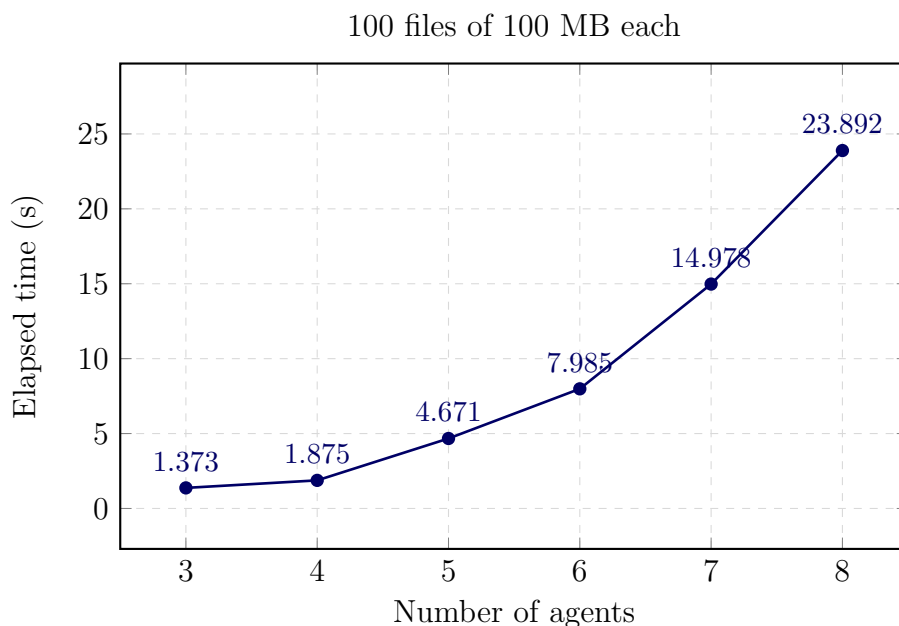


Figure 4.2: Elapsed time for the corruption check with 100 files of 100 MB each, with all agents online. Each agent stores $100 \times (100 \text{ MB} / \text{number of agents})$ of data.

Test 2: Many small files, all agents online The second test involved 10,000 files of 1 MB each, maintaining the same total dataset size of 10 GB. This scenario highlights the impact of a high file count relative to file size. As shown in Figure 4.3, elapsed time increases substantially with the number of agents, from 0.469 seconds with 3 agents to 81.032 seconds with 8 agents. The growth compared to Test 1 indicates that the number of files significantly influences corruption check performance, primarily due to the overhead of managing numerous small shards.

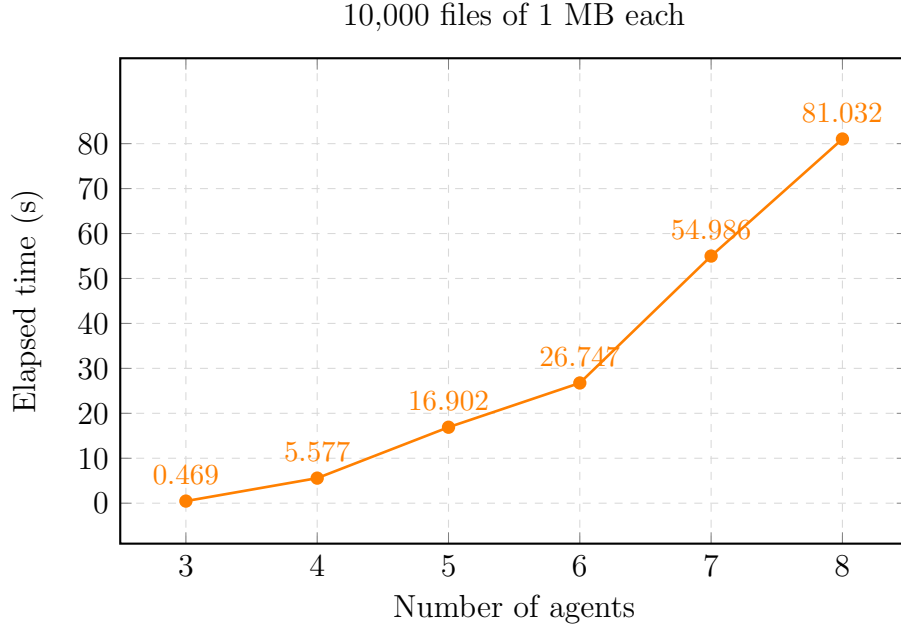


Figure 4.3: Elapsed time for the corruption check with 10,000 files of 1 MB each, with all agents online. Each agent stores $10,000 \times (1 \text{ MB} / \text{number of agents})$ of data.

Test 3: Large files, but small dataset This test evaluates system performance on a small dataset consisting of 10 files, each 1 GB in size, under different cluster sizes. All agents remained online during the corruption check. Figure 4.4 shows the elapsed time as the number of agents increases from 3 to 8. As expected, the elapsed time grows with the number of agents, mainly due to increased network communication overhead and coordination between nodes.

Interestingly, even though the total dataset size (10 GB) is comparable to Tests 1 and 2, the overall elapsed time is significantly lower. This suggests that the system handles a smaller number of large files more efficiently than many smaller files. This behavior could indicate that the corruption check mechanism scales better with file size than with file count.

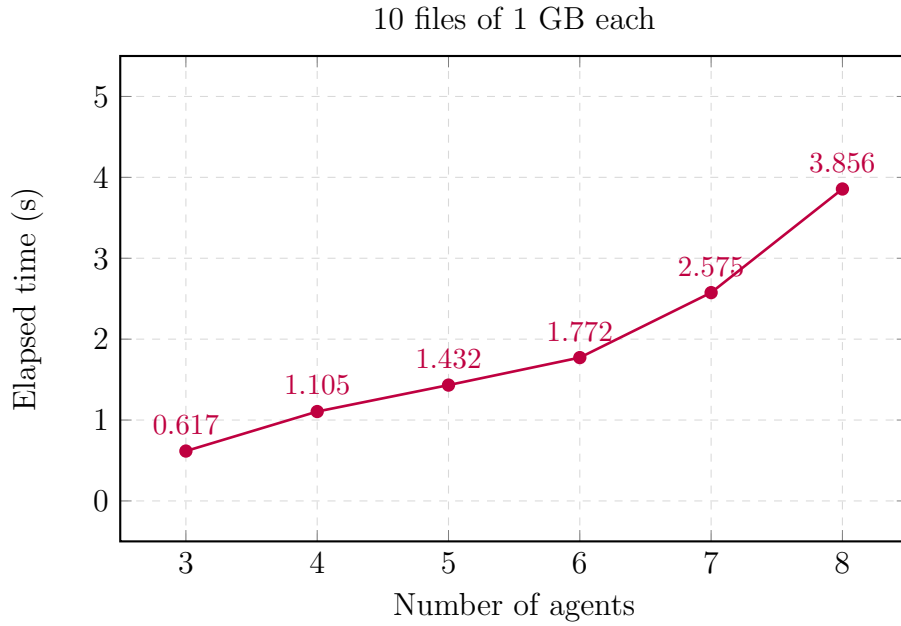


Figure 4.4: Elapsed time for the corruption check with 10 files of 1 GB each, with all agents online. Each agent stores $10 \times (1 \text{ GB}/\text{number of agents})$ of data.

Test 4: Small files, partially offline agents The fourth scenario evaluates the effect of offline agents. 1,000 files of 150 KB each were uploaded, and elapsed time was measured both with all agents online and with a subset of agents offline during the corruption check. Figure 4.5 compares the two configurations. Offline agents introduce additional latency due to the timeout before retrieving the previous saved hash, with elapsed times ranging from 28.2 to 91.338 seconds, compared to 3.1 to 69.221 seconds when all agents are online.

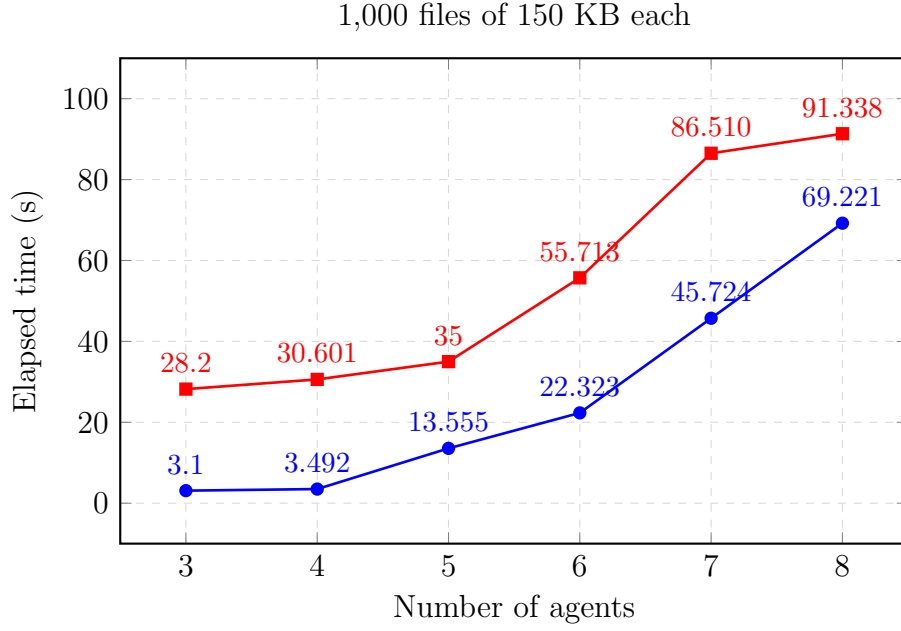


Figure 4.5: Elapsed time of the corruption check with 1,000 files, each 150 KB in size. Each agent stores $1,000 \times (150 \text{ KB} / \text{number of agents})$ of data. In blue with none offline agents; in red with offline agents.

Test 5: Very large number of tiny files The last test evaluates system performance with an extremely large number of very small files. The dataset consisted of one million files, distributed across different cluster configurations. Unlike the previous tests, where file sizes varied with the number of agents, in this case each file had a fixed size of 4 KB. Consequently, increasing the number of agents also increases the total global dataset size, allowing an assessment of how the system handles both a high file count and a growing overall workload.

Figure 4.6 shows the total elapsed time for the corruption check as the number of agents increases. Despite the large file count, the system maintains acceptable performance, with time increasing gradually as more agents participate. This behavior highlights the scalability of the corruption check mechanism, which efficiently verifies tasks across nodes. However, the absolute elapsed time is significantly higher than in previous tests with fewer, larger files, reinforcing that per-file management overhead dominates when processing millions of small files. The test demonstrates that while the system remains operationally robust, optimizing metadata handling and batching operations could further improve scalability for dataset dominated by small files.

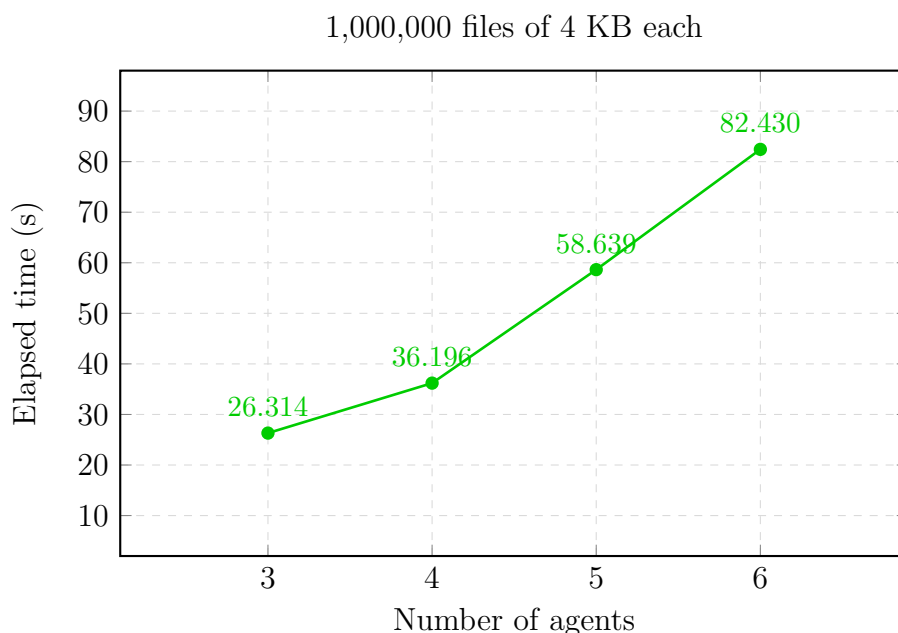


Figure 4.6: Elapsed time for corruption check on very large datasets. The total dataset size increases with the number of agents: 12 GB for 3 agents, 16 GB for 4 agents, 20 GB for 5 agents, and 24 GB for 6 agents. Each agent stores 4 GB of data.

Results The experimental evaluation demonstrates that the system maintains correctness and functional reliability across a wide variety of scenarios. However, performance degrades as the cluster size increases, primarily due to the coordination and communication overhead introduced by the Raft consensus, as well as the computational cost of Merkle tree operations and network latency when retrieving root hashes from agents.

In Test 1, with 100 files of 100 MB each (10 GB total), the elapsed time increased from 1.37 seconds with 3 agents to 23.89 seconds with 8 agents. This trend shows that the system remains functional but becomes progressively slower as coordination overhead grows.

In Test 2, using 10,000 files of 1 MB each (10 GB total), elapsed time increased from 0.47 seconds with 3 agents to 81.03 seconds with 8 agents. This represents about 170x increase, clearly showing that scenarios with many small files amplify the cost of synchronization and consensus, leading to diminishing performance returns as the cluster expands.

Test 3, with 10 files of 1 GB each (10 GB total), exhibited a milder increase (from 0.62 seconds to 3.86 seconds) indicating that the system handles large files more efficiently. Compared to Tests 1 and 2, this suggests that performance loss is primarily driven by the number of files (and resulting coordination steps), not by total data size.

In Test 4, with 1,000 files of 150 KB each (150 MB total), the system was evaluated under partial node unavailability. When some agents were offline, execution time increased by roughly 9x (for example, from 3.1 seconds to 28.2 seconds with 3 agents). However, the relative slowdown diminished with larger clusters, confirming that Raft’s fault-tolerant synchronization mitigates the effects of offline nodes, albeit at a cost in latency.

Finally, Test 5, involving one million files of 4 KB each, measured total processing time from 26.31 seconds to 82.43 seconds as dataset size grew from 12 GB to 24 GB. Despite the large number of files, absolute latency grows and the system continues to process data at a predictable rate.

Overall, the results show that the system is robust but not performance-scalable. It preserves data integrity and correctness under varying dataset and node conditions, but verification time increases disproportionately with the number of agents and files. These findings highlight the trade-off between distributed consistency and performance in consensus-based integrity verification protocols.

5 Conclusion

This thesis presented the design and implementation of a Merkle-tree-based integrity verification protocol for geo-distributed storage systems. The proposed system integrates Merkle trees, the Raft consensus algorithm, and Reed-Solomon coding to provide a reliable corruption detection mechanism that remains functional even when some agents are temporarily offline.

The developed prototype demonstrated that it is possible to maintain a consistent and verifiable integrity state across distributed agents without relying on full file scans or constant node availability. Raft ensures that integrity metadata is synchronized cluster-wide, while Merkle trees allow hierarchical and efficient integrity checks at the folder or subfolder level.

The experimental results confirmed the correctness and resilience of the approach under different scenarios and network conditions. However, the tests also revealed a clear performance limitation: verification time increases as the number of agents grows, mainly due to consensus and communication overhead. The system remains functionally correct but becomes slower in larger clusters, particularly in scenarios with many small files, where metadata synchronization dominates the cost.

Despite this, the proposed architecture fulfills its primary objective: enabling fault-tolerant, verifiable, and consistent corruption detection in distributed environments. Its design makes it extensible to new optimizations and deployment models.

Future Work and Considerations Several directions emerge for further research and practical refinement:

- **Adaptive Merkle tree deployment per customer.** Since corruption checks behave differently depending on filesystem organization, the system could apply Merkle trees adaptively based on customer usage. Some customers store many small files, while others handle few but very large files. Maintaining a dedicated filesystem per customer (for each agent) would also

improve security and isolation, avoiding shared-state interference between unrelated datasets.

- **Scalability to a large number of agents.** Current experiments were limited to small clusters. It remains to be tested how the system behaves with several dozens of agents. If corruption checks require hours to complete, the approach could become impractical at large scale; therefore, performance profiling for large clusters is essential.
- **Optimizing folder and hash map access.** The use of `TrieMap`, potentially in a concurrent implementation, could optimize lookup speed for subfolders in `hashes2`, reducing blocking time during verification.
- **Reducing redundant root retrievals.** Some performance gain might be achieved by avoiding unnecessary *get root* operations, retrieving roots randomly or selectively. However, this introduces the risk of inconsistency or false negatives, so the safest approach remains to always query the current Merkle root from all online agents.
- **Parallel verification of independent folders.** Each top-level folder is independent; therefore, Merkle root verification can be executed concurrently across top-level directories. This parallelism could significantly reduce total verification time without compromising correctness.
- **Deeper folder hierarchies.** The current two-level folder model simplifies testing but may limit scalability. Adding additional folder levels could further localize corruption checks and reduce recomputation overhead, potentially improving performance for large and complex filesystems.
- **Integration with Cubbit’s file versioning system.** Cubbit’s versioning mechanism already allows users to restore previous file states. This feature implicitly extends the proposed protocol, enabling a combined repair and verification process: the system can revert to a prior version of a file or folder and then perform a corruption check, providing an additional safeguard against data loss.
- **Folder-level verification granularity.** The current protocol operates at the folder level rather than on individual files. As a result, while it can detect that a folder contains corrupted data, it cannot directly identify which specific file within that folder is affected. Future developments could explore finer-grained verification to pinpoint corrupted files more precisely.

In summary, this work shows that a Merkle-tree-based integrity verification protocol coordinated through Raft can provide strong correctness and resilience guarantees for geo-distributed storage. Although performance decreases with larger clusters, the approach remains a robust foundation for future distributed integrity systems. With targeted optimizations, this proposed integrity verification protocol could evolve into a practical and efficient solution for production-scale environments such as Cubbit.

Bibliography

- [1] Peter M Chen, Edward K Lee, Garth A Gibson, Randy H Katz, and David A Patterson. Raid: High-performance, reliable secondary storage. *ACM Computing Surveys (CSUR)*, 26(2):145–185, 1994.
- [2] Ralph C Merkle. A certified digital signature. In *Conference on the Theory and Application of Cryptology*, pages 218–238. Springer, 1989.
- [3] Ivan Bjerre Damgård. Collision free hash functions and public key signature schemes. In *Workshop on the Theory and Application of Cryptographic Techniques*, pages 203–216. Springer, 1987.
- [4] Merkle tree in bitcoin. <https://bitcoinwiki.org/wiki/merkle-tree>. Accessed: 2025-09-02.
- [5] Patricia merkle trie in ethereum. <https://ethereum.org/en/developers/docs/data-structures-and-encoding/patricia-merkle-trie/>. Accessed: 2025-09-02.
- [6] Merkle directed acyclic graphs in ipfs. <https://docs.ipfs.tech/concepts/merkle-dag/>. Accessed: 2025-09-02.
- [7] Giuseppe DeCandia, Deniz Hastorun, Madan Jampani, Gunavardhan Kakulapati, Avinash Lakshman, Alex Pilchin, Swaminathan Sivasubramanian, Peter Voshall, and Werner Vogels. Dynamo: Amazon’s highly available key-value store. *ACM SIGOPS operating systems review*, 41(6):205–220, 2007.
- [8] Johannes Buchmann, Erik Dahmen, and Andreas Hülsing. Xmss-a practical forward secure signature scheme based on minimal security assumptions. In *International Workshop on Post-Quantum Cryptography*, pages 117–129. Springer, 2011.
- [9] Johannes Buchmann, Erik Dahmen, and Michael Schneider. Merkle tree traversal revisited. In *International Workshop on Post-Quantum Cryptography*, pages 63–78. Springer, 2008.

- [10] Wouter Penard and Tim Van Werkhoven. On the secure hash algorithm family. *Cryptography in context*, pages 1–18, 2008.
- [11] Guido Bertoni, Joan Daemen, Michaël Peeters, and Gilles Van Assche. Kccak. In *Annual international conference on the theory and applications of cryptographic techniques*, pages 313–314. Springer, 2013.
- [12] Nist selects winner of secure hash algorithm (sha-3) competition. <https://www.nist.gov/news-events/news/2012/10/nist-selects-winner-secure-hash-algorithm-sha-3-competition>. Accessed: 2025-09-07.
- [13] Jack O’Connor, Jean-Philippe Aumasson, Samuel Neves, and Zooko Wilcox-O’Hearn. Blake3: one function, fast everywhere. *url: https://github.com/BLAKE3-team/BLAKE3-specs/blob/master/blake3.pdf*, 2021.
- [14] Jean-Philippe Aumasson, Samuel Neves, Zooko Wilcox-O’Hearn, and Christian Winnerlein. Blake2: simpler, smaller, fast as md5. In *International Conference on Applied Cryptography and Network Security*, pages 119–135. Springer, 2013.
- [15] Shay Gueron, Simon Johnson, and Jesse Walker. Sha-512/256. In *2011 Eighth International Conference on Information Technology: New Generations*, pages 354–358. IEEE, 2011.
- [16] Diego Ongaro and John Ousterhout. In search of an understandable consensus algorithm. *url: https://raft.github.io/raft.pdf*, 2014.
- [17] etcd performance. <https://etcd.io/docs/v3.6/op-guide/performance/>. Accessed: 2025-09-03.
- [18] Raft use in tikv. <https://tikv.org/deep-dive/consensus-algorithm/raft/>. Accessed: 2025-09-03.
- [19] Leslie Lamport, Robert Shostak, and Marshall Pease. The byzantine generals problem. *ACM Trans. Program. Lang. Syst.*, 4(3):382–401, July 1982.
- [20] Matteo Monti, Martina Camaioni, and Pierre-Louis Roman. Fast leaderless byzantine total order broadcast. *arXiv preprint arXiv:2412.14061*, 2024.
- [21] Miguel Castro, Barbara Liskov, et al. Practical byzantine fault tolerance. In *OsDI*, volume 99, pages 173–186, 1999.

- [22] Haoran Shi, Zehua Chen, Yongqiang Cheng, Xiaofeng Liu, and Qianqian Wang. Pb-raft: A byzantine fault tolerance consensus algorithm based on weighted pagerank and bls threshold signature. *Peer-to-Peer Networking and Applications*, 18(1):26, 2025.
- [23] Dan Boneh, Ben Lynn, and Hovav Shacham. Short signatures from the weil pairing. In *International conference on the theory and application of cryptology and information security*, pages 514–532. Springer, 2001.
- [24] Irving S Reed and Gustave Solomon. Polynomial codes over certain finite fields. *Journal of the society for industrial and applied mathematics*, 8(2):300–304, 1960.
- [25] Organizing a go module. <https://go.dev/doc/modules/layout>. Accessed: 2025-10-01.

List of Figures

2.1	Merkle tree authentication path for $data_1$. Leaves are hashed as $node_i = f(data_i)$, and internal nodes are computed as $f(node_{\text{left}} node_{\text{right}})$ (Equation 2.1). The proof requires only the sibling nodes $\{node_0, node_{23}\}$ to recompute the root.	9
2.2	Single-threaded throughput of BLAKE3 and other hash functions on an AWS c5.metal instance, measured in cycles per byte (cpb). Lower values indicate fewer CPU cycles needed per byte.	14
2.3	Hashing speed comparison of BLAKE3 and other hash functions on an AWS c5.metal instance with a 16 KiB input, using a single thread. Higher values (MiB/s) indicate faster processing.	15
2.4	Server states. Followers only respond to requests from other servers. If a follower receives no communication, it becomes a candidate and initiates an election. A candidate that receives votes from a majority of the full cluster becomes the new leader. Leaders typically operate until they fail.	16
3.1	An example of a binary Merkle tree with 4 leaves, showing the different levels: leaves (Level 1), internal nodes (Level 2), and the root (Level 3).	23
3.2	organization of files under the folder ff , represented as a tree structure.	28
3.3	Extended example of file organization under ff , represented as a tree structure with multiple files.	29
3.4	Example of filesystems for Agent 1 , Agent 2 , and Agent 3	31
3.5	Merkle tree constructed from the root hashes of top-level folders. Each folder root acts as a leaf in this Merkle tree.	32
3.6	Merkle tree constructed from the root hashes of second-level folders. Each folder root acts as a leaf in this Merkle tree.	32
3.7	Sequence diagram for uploading a file. In this example, Agent 1 is the Raft leader and the uploaded file has a path starting with ff/4c	35

3.8	Sequence diagram illustrating the Corruption Check process for the top-level folder ff . Agent 1 is the Raft leader.	37
3.9	Corruption check process for the top-level folder ff , considering some agents may be offline.	40
4.1	Interaction between Go and Rust components. The Go merkletree module invokes the Rust binary via exec.Command , which delegates computation to the Rust Merkle tree library.	49
4.2	Elapsed time for the corruption check with 100 files of 100 MB each, with all agents online. Each agent stores $100 \times (100 \text{ MB} / \text{number of agents})$ of data.	51
4.3	Elapsed time for the corruption check with 10,000 files of 1 MB each, with all agents online. Each agent stores $10,000 \times (1 \text{ MB} / \text{number of agents})$ of data.	52
4.4	Elapsed time for the corruption check with 10 files of 1 GB each, with all agents online. Each agent stores $10 \times (1 \text{ GB} / \text{number of agents})$ of data.	53
4.5	Elapsed time of the corruption check with 1,000 files, each 150 KB in size. Each agent stores $1,000 \times (150 \text{ KB} / \text{number of agents})$ of data. In blue with none offline agents; in red with offline agents. . .	54
4.6	Elapsed time for corruption check on very large datasets. The total dataset size increases with the number of agents: 12 GB for 3 agents, 16 GB for 4 agents, 20 GB for 5 agents, and 24 GB for 6 agents. Each agent stores 4 GB of data.	55

List of Tables

2.1	Merkle tree benchmarks with 10 nodes per dataset size (5 MB, 10 MB, and 15 MB).	15
4.1	Specifications of the machines used in the testing environment. . . .	50

Acknowledgments

I would like to express my gratitude to my supervisor, Professor Özalp Babaoğlu, for the support he provided throughout the development of this thesis.

I am also thankful to the Cubbit team for the ideas and inspiration that contributed to this work.

Finally, my deepest thanks go to Claudia. I would not be where I am without you.

A Listings

A.1 Protobuf definition for Agent service

```
1  service Agent {
2      rpc SendShard(ShardRequest) returns (ShardResponse) {}
3      rpc GetShard(ShardGetRequest) returns (ShardGetResponse) {}
4      rpc AckShard(ShardAckRequest) returns (ShardAckResponse) {}
5      rpc GetRootHash(RootHashRequest) returns (RootHashResponse) {}
6      rpc JoinRaft(JoinRequest) returns (JoinResponse) {}
7  }
8
9  message ShardRequest {
10     string filename = 1; int64 index = 2; bytes data = 3;
11 }
12
13 message ShardGetRequest {
14     string filename = 1; int64 index = 2;
15 }
16
17 message ShardAckRequest {
18     string filename = 1; int64 index = 2; bytes roots = 3;
19 }
20
21 message ShardResponse {
22     string filename = 1; bytes salt = 2;
23 }
24
25 message ShardGetResponse { bytes data = 1; }
26 message ShardAckResponse { bool status = 1; }
27 message RootHashRequest { bytes folder = 1; }
28 message RootHashResponse { bytes hash = 1; }
29 // ...
```

Listing 14: Protobuf definitions for the `Agent` service, used for communication between gateways and agents, as well as among agents themselves. The file is located in `internal/proto/agent.proto`.

A.2 Gateway Upload Handler Implementation

```
1 func UploadHandler(w http.ResponseWriter, r *http.Request) {
2     // Open the file in byte format.
3     // Generate a key and encrypt the file with it.
4     // Encrypt the local file using a random key.
5     ciphertext, err := cryptography.Enc(file, key)
6
7     // Create N+K shards from the encrypted file ([][]byte).
8     shardBytes, err := reedSolomon.Create(N, K, ciphertext)
9
10    // Generate a "good" salt to extend the filename.
11    // Send each shard to a different agent.
12    for i, shard := range shardBytes {
13        resp, err := rpc.SendShard(
14            cfg.Agents[i], filename+salt, i, shard,
15        )
16
17        if err != nil {
18            // Handle error
19        }
20    }
21
22    // Build a JSON response for the client.
23    jsonResponse, _ := json.Marshal(/* ... */)
24
25    w.Header().Set("Content-Type", "application/json")
26    w.Write(jsonResponse)
27 }
28
```

Listing 15: Upload handler: Gateway orchestrates file encryption, Reed-Solomon shard creation, and transmission to agents via the `rpc.SendShard` wrapper.

A.3 SendShard RPC Wrapper Implementation

```
1 func SendShard(agent, filename string, index int,
2   data []byte) (*pb.ShardResponse, error) {
3   dialCtx, dialCancel :=
4     context.WithTimeout(context.Background(), 100*time.Millisecond)
5   defer dialCancel()
6
7   conn, _ := grpc.DialContext(dialCtx, agent,
8     grpc.WithTransportCredentials(insecure.NewCredentials()),
9     grpc.WithBlock())
10  defer conn.Close()
11
12  // Instantiate the gRPC client for the Agent service.
13  c := pb.NewAgentClient(conn)
14
15  ctx, cancel := context.WithTimeout(context.Background(), time.Second)
16  defer cancel()
17
18  // Call the SendShard procedure for the i-th shard of the file.
19  resp, _ := c.SendShard(ctx, &pb.ShardRequest{
20    Filename: filename, Index: int64(index), Data: data,
21  })
22
23  return resp, nil
24 }
```

Listing 16: SendShard wrapper: intermediate function that establishes a gRPC connection to the target Agent, forwards the shard data to the generated gRPC client stub in `agent_grpc.pb.go`, and returns the response.

A.4 Gateway Download Handler Implementation

```
1 func DownloadHandler(w http.ResponseWriter, r *http.Request) {
2     // Retrieve the salt for a given filename
3     // to reconstruct the exact file saved on agents.
4     endFile := getEndFile(filename, salt)
5
6     // Retrieve all shards from agents
7     shards, _ := rpc.GetAllShards(endFile)
8
9     // Reconstruct the entire file using Reed-Solomon,
10    // and store it at endFile path
11    _ = reedSolomon.Reconstruct(cfg.N, cfg.K, endFile, shards)
12    // Decrypt the reconstructed file and store it as filename
13
14    // Return the plaintext file as an attachment
15    w.Header()
16        .Set("Content-Disposition",
17            fmt.Sprintf("attachment; filename=%s", filename),
18        )
19    content, _ = ioutil.ReadFile(filename)
20
21    // Handle possible errors and clear temporary files
22
23    w.Write(content)
24 }
```

Listing 17: Download handler: logic that retrieves all shards of a file via the `rpc.GetAllShards` wrapper, reconstructs the file using Reed-Solomon, decrypts it, and returns it as a download to the user.

A.5 Agent Service Initialization and gRPC Server Setup

```
1 import (
2     pb "<path_with_proto_files>"
3     // ...
4 )
5
6 // Server implements the gRPC service defined in the Protobuf file.
7 type Server struct {
8     pb.UnimplementedAgentServer
9     RaftServer *raft.Server
10    // Other fields
11 }
12
13 s := grpc.NewServer()
14 reflection.Register(s)
15 server := server.Server{}
16
17 // Register the gRPC server with the generated Protobuf bindings.
18 pb.RegisterAgentServer(s, &server)
19
20 server.RaftServer = newRaft(ctx, ..., ..., ..., ...)
21
22 lis, _ := net.Listen("tcp", uri)
23 s.Serve(lis)
```

Listing 18: Agent service startup. The gRPC server is initialized and registered, and the node joins or bootstraps a Raft cluster.

A.6 Raft Node Initialization

```
1 import (
2     "github.com/hashicorp/raft"
3     boltdb "github.com/hashicorp/raft-boltdb"
4     // ...
5 )
6
7 func newRaft(ctx context.Context, bootstrap bool, id, raftAddress string,
8     fsm raft.FSM) (*raft.Raft, *raft.NetworkTransport, error) {
9     conf := raft.DefaultConfig()
10    conf.LocalID = raft.ServerID(id)
11
12    // Define the base directory for Raft persistence.
13
14    logs, _ := boltdb.NewBoltStore(filepath.Join(baseDir, "logs.dat"))
15    stable, _ := boltdb.NewBoltStore(filepath.Join(baseDir, "stable.dat"))
16    snaps, _ := raft.NewFileSnapshotStore(baseDir, 3, os.Stderr)
17
18    addr, _ := net.ResolveTCPAddr("tcp", raftAddress)
19    transport, _ := raft.NewTCPTransport(
20        raftAddress, addr, 3, 10*time.Second, os.Stderr)
21
22    r, _ := raft.NewRaft(conf, fsm, logs, stable, snaps, transport)
23
24    if bootstrap {
25        cfg := raft.Configuration{
26            Servers: []raft.Server{{
27                ID:      conf.LocalID,
28                Address: transport.LocalAddr(),
29            }},
30        },
31    }
32    _ = r.BootstrapCluster(cfg).Error()
33 }
34
35 return r, transport, nil
36 }
```

Listing 19: Partial implementation of the `newRaft` function, which initializes the Raft consensus node.

A.7 Client-Side Raft Join Request

```
1 // Establish a connection to a Raft member.
2 dialCtx, dialCancel := context.WithTimeout(context.Background(),
3                                           100*time.Millisecond)
4 defer dialCancel()
5
6 conn, err := grpc.DialContext(dialCtx, "<url-of-Raft-member-to-join>",
7                               grpc.WithTransportCredentials(insecure.NewCredentials()),
8                               grpc.WithBlock())
9
10 c := pb.NewAgentClient(conn)
11
12 // Send a JoinRaft request with the new node's ID and Raft address.
13 ctx, cancel := context.WithTimeout(context.Background(), time.Second)
14 defer cancel()
15
16 _, err = c.JoinRaft(ctx, &pb.JoinRequest{
17     Address: raftAddress, // Address such as 0.0.0.0:4002
18     Id:      node, // Identifier such as nodeB
19 })
```

Listing 20: Client-side gRPC call to join an existing Raft cluster. The joining agent dials a Raft member and invokes the `JoinRaft` RPC with its address and identifier.

A.8 Server-Side Raft Join Handler

```
1 func (s *Server) JoinRaft(ctx context.Context,
2     in *pb.JoinRequest) (*pb.JoinResponse, error) {
3     address := in.GetAddress()
4     id := in.GetId()
5
6     // Attempt to add the new server to the Raft cluster.
7     if err := join(s.RaftServer, id, address); err != nil {
8         // Handle error
9     }
10
11     return &pb.JoinResponse{}, nil
12 }
13
14
15 // If a server with the same ID or address already exists, it is removed before
16 // the new server is added as a voter.
17 func join(r *raft.Raft, nodeId, addr string) error {
18     configFuture := r.GetConfiguration()
19
20     for _, srv := range configFuture.Configuration().Servers {
21         if srv.ID == raft.ServerID(nodeId) ||
22             srv.Address == raft.ServerAddress(addr) {
23             if srv.ID == raft.ServerID(nodeId) &&
24                 srv.Address == raft.ServerAddress(addr) {
25                 return nil
26             }
27             // Remove the existing server before re-adding.
28             _ = r.RemoveServer(srv.ID, 0, 0)
29         }
30     }
31
32     // Add the new server as a voting member of the Raft cluster.
33     f := r.AddVoter(raft.ServerID(nodeId), raft.ServerAddress(addr), 0, 0)
34     if f.Error() != nil {
35         return f.Error()
36     }
37     return nil
38 }
```

Listing 21: Server-side handler for JoinRaft. The bootstrap node receives a join request and updates the Raft cluster configuration by invoking the join helper function.

A.9 Server-Side SendShard Handler

```
1 func (s *Server) SendShard(ctx context.Context,
2   in *pb.ShardRequest) (*pb.ShardResponse, error) {
3   fname := in.GetFilename()
4   index := in.GetIndex()
5   data := in.GetData()
6   filename := fname[:len(fname)-2]
7   salt := fname[len(fname)-2:]
8
9   go func() {
10    // Compute top-level and second-level folder roots
11    rootLvl1, _ := merkletree.FolderRootHash(path.folderLvl1)
12    rootLvl2, _ := merkletree.FolderRootHash(path.folderLvl2)
13
14    // Prepare the acknowledgement message including both roots
15    req := &pb.ShardAckRequest{
16      Filename: filename + salt,
17      Index:    int64(index),
18      Roots:    append(rootLvl1, rootLvl2...),
19    }
20
21    // Forward the roots to the leader or process locally
22    // if this node is the leader
23    if s.Store.Raft.State() == raft.Leader {
24      _, err = s.AckShard(ctx, req)
25    } else {
26      _, err = c.AckShard(ctx, req)
27    }
28  }()
29
30  return &pb.ShardResponse{Filename: path, Salt: []byte(salt)}, nil
31 }
```

Listing 22: Server-side handler for `SendShard`. Retrieves folder roots, stores the shard locally, and forwards root information to the Raft leader.

A.10 Server-Side GetShard Handler

```
1 func (s *Server) GetShard(ctx context.Context,  
2 in *pb.ShardGetRequest) (*pb.ShardGetResponse, error) {  
3     filename := in.GetFilename()  
4     index := in.GetIndex()  
5  
6     // Resolve the actual path of the requested shard  
7     f, _ := os.Open(path)  
8     content, _ := ioutil.ReadAll(f)  
9  
10    return &pb.ShardGetResponse{Data: content}, nil  
11 }
```

Listing 23: Server-side handler for GetShard. Retrieves the requested shard from local storage and returns its content.

A.11 Raft Log Command Structure

```
1 const (  
2     UploadAck OpCode = iota // Acknowledge the successful storage of a shard  
3     StoreRootHash // Store a Merkle tree root hash  
4     StoreAgentHash // Store a Merkle tree hash for a specific agent  
5     SignalCorruption // Store the corruption status of a folder  
6 )  
7  
8 type Command struct {  
9     Code OpCode `json:"code"`  
10    Action interface{} `json:"action"`  
11 }
```

Listing 24: Command definition used for Raft log entries. Each command is identified by an opcode and carries an action payload.

A.12 Server-Side AckShard Handler

```
1 func (s *Server) AckShard(ctx context.Context,
2   in *pb.ShardAckRequest) (*pb.ShardAckResponse, error) {
3   filename := in.GetFilename()
4   index := in.GetIndex()
5   agentHashes := in.GetRoots()
6
7   // Split concatenated roots into two 32-byte values
8   agentRoots := [][]byte{agentHashes[:64], agentHashes[64:]}
9
10  // Mark the shard as acknowledged
11  done := make([]bool, N+K)
12  done[index] = true
13  shardAcknowledge(s.RaftServer, filename, done)
14
15  path := ... // Retrieve the final path
16  toplevel := path.folderLvl1
17  secondlevel := path.folderLvl2
18
19  // Store per-agent Merkle roots
20  saveAgentHash(s.RaftServer, index,
21    [][]byte{toplevel, secondlevel}, agentRoots)
22
23  // Compute and store global Merkle roots for the folders
24  root1, _ := merkletree.RootHash(hashes1[toplevel])
25  root2, _ := merkletree.RootHash(hashes2[secondlevel])
26  saveRoot(s.RaftServer, [][]byte{toplevel, secondlevel},
27    [][]byte{root1, root2})
28
29  return &pb.ShardAckResponse{Status: true}, nil
30 }
```

Listing 25: Server-side handler for AckShard. Updates shard acknowledgments, stores per-agent hashes, and records Merkle roots in the Raft log.

A.13 Raft Log Entry Helper Functions

```
1 func shardAcknowledge(r raft.Server, filename string, done []bool) error {
2     c := Command{
3         Code: UploadAck,
4         Action: ShardDone{ Filename: []byte(filename), Done: done },
5     }
6
7     raftRequestData, _ := json.Marshal(c)
8     return r.Apply([]byte(raftRequestData), 1*time.Second).Error()
9 }
10
11 func saveRoot(r raft.Server, folders [][]byte, hashes [][]byte) error {
12     c := Command{
13         Code: StoreRootHash,
14         Action: MerkleTreeRootHash{ Folder1: folders[0], RootHash1: hashes[0],
15                                 Folder2: folders[1], RootHash2: hashes[1] },
16     }
17
18     raftRequestData, _ := json.Marshal(c)
19     return r.Apply([]byte(raftRequestData), 1*time.Second).Error()
20 }
21
22 func saveAgentHash(r raft.Server, agentId int64, folders [][]byte,
23 hashes [][]byte) error {
24     c := Command{
25         Code: StoreAgentHash,
26         Action: MerkleTreeHash{
27             AgentId: agentId, Folder1: folders[0], AgentHash1: hashes[0],
28             Folder2: folders[1], AgentHash2: hashes[1] },
29     }
30
31     raftRequestData, _ := json.Marshal(c)
32     return r.Apply([]byte(raftRequestData), 1*time.Second).Error()
33 }
```

Listing 26: Helper functions for applying shard acknowledgments, Merkle roots, and per-agent hashes to the Raft log.

A.14 Merkle Tree Creation in Rust

```
1 let tree = if args.file {
2     MerkleTree::from_paths(hasher, args.args)
3 } else {
4     let data: Vec<Vec<u8>> = args.args.into_iter()
5         .map(|s| s.into_bytes()).collect();
6     MerkleTree::new(hasher, data)
7 };
8
9 println!("{}", tree.root().hash());
```

Listing 27: Partial implementation of the Rust binary for Merkle tree creation.

A.15 Merkle Proof Verification in Rust

```
1 if let Some(root_hash) = args.proof {
2     let nodes = // Build nodes from folders or raw data ...
3     let first_node = nodes[0].clone();
4     let proofer = DefaultProofer::new(hasher, nodes);
5     let proof = proofer.generate(0).expect("Couldn't generate proof");
6     let verified = proofer.verify_hash(
7         &proof, first_node.hash().to_string(), &root_hash[..]
8     );
9     println!("{}", verified);
10 } else {
11     // Merkle tree creation...
12 }
```

Listing 28: Extension of the Rust binary for Merkle proof verification.

A.16 Merkle Tree Module Prototypes (Go)

```
1 // Verify a Merkle tree proof for some `hashes` with a `rootHash`.
2 func Verify(hashes [][]byte, rootHash []byte) bool { ... }
3
4 // Returns the root hash of the Merkle tree generated for a folder in `path`
5 func FolderRootHash(path string) ([]byte, error) { ... }
6
7 // Returns the root hash of the Merkle tree generated for a list of data
8 func RootHash(data [][]byte) ([]byte, error) { ... }
```

Listing 29: Prototypes of the merkletree Go module.

A.17 Corruption Check Algorithm

```
1  for folder1, agentHashes1 := range hashes1 {
2      root1 := roots1[folder1]
3      data := // Retrieve roots for folder1 using agentHashes1 (backup if needed)
4      isCorrupted := merkleTree.IsPathCorrupted(data, root1)
5
6      if isCorrupted {
7          for folder2, agentHashes2 := range hashes2 {
8              if strings.HasPrefix(folder2, folder1) {
9                  root2 := roots2[folder2]
10                 data := // Retrieve roots for folder2 using agentHashes2
11                 isCorruptedLevel2 := merkleTree.IsPathCorrupted(data, root2)
12
13                 if isCorruptedLevel2 {
14                     saveCorruptionState(s.RaftServer, folder2, true)
15                 } else if corruptions[folder2] {
16                     // Folder no longer corrupted, but other subfolders may be.
17                     saveCorruptionState(s.RaftServer, folder2, false)
18                 }
19             }
20         }
21         saveCorruptionState(s.RaftServer, folder1, true)
22     } else if corruptions[folder1] {
23         // Update corruption status for the top-level folder
24         // and its second-level children.
25     }
26 }
```

Listing 30: Partial implementation of the corruption check algorithm. The leader verifies Merkle proofs at both top-level and second-level folders, and signals corruption states through the Raft log.